Petrology and geochemistry of scandium in New Caledonian Ni-Co laterites

Y. Teitler, M. Cathelineau, M. Ulrich, J. P. Ambrosi, Manuel Munoz, B. Sevin

Petrology and geochemistry of scandium in New Caledonian Ni-Co laterites

Y. TEITLER[1]*, M. CATHELINEAU[1], M. ULRICH[2], J.P AMBROSI[3], M. MUNOZ[4]

[1]Laboratoire GéoRessources, rue Jacques Callot, BP 70239, 54506 Vandoeuvre-lès-Nancy Cedex, France

[2]EOST, 1 rue Blessig, 67084 Strasbourg Cedex, France

[3]CEREGE, AMU,CNRS,IRd, INRA, CdF, Technopôle de l'Arbois-Méditerranée, BP80, 13545 Aix en Provence cedex 4

[4]Géosciences Montpellier, place Eugène Bataillon, 34095 Montpellier cedex 05, France

*yoram.teitler@univ-lorraine.fr

Declarations of interest: none

Keywords

Scandium, laterite, Ni-laterite, goethite, New Caledonia

Abstract

The growing demand for scandium (Sc), essential for several modern industrial applications, thrives the mining industry to develop alternative Sc sources. In such context, significant Sc concentrations (~100 ppm) were recently reported in several Ni-Co lateritic oxide ores developed after mafic-ultramafic rocks. This contribution examines the distribution of Sc in Ni-Co laterites from New Caledonia, the sixth largest Ni producer worldwide. Representative lateritic profiles were selected based on the protolith type and include dunite, harzburgite and lherzolite protoliths, wherein the Sc content, determined by the relative proportion of olivine and pyroxene, ranges from <5 ppm in dunite to >10 ppm in lherzolite.

In Ni-Co laterites, dissolution and leaching of primary Mg-rich silicates leads to the residual enrichment of iron as ferric oxides/oxyhydroxides in the upper horizons. Downward remobilisation and trapping of Ni and Co lead to their local enrichment to economic concentrations, with maximum grades reached in the rocky saprolite and in the transition laterite

horizons, respectively. In contrast, maximum Sc enrichment occurs in the yellow laterite horizon, where Sc-bearing goethite reaches about ten times the Sc content of the parent rock. Consequently, harzburgite- and lherzolite-derived yellow laterites yield maximum Sc concentrations up to 100 ppm, together with moderate Ni and Co concentrations. There, Sc is a potentially valuable by-product that could be successfully co-extracted along with Ni and Co through hydrometallurgical processing.

In addition to peridotite-hosted laterites, hornblende-rich amphibolites yield elevated Sc up to 130 ppm. The saprolitisation of amphibolites leads to the formation of a goethite-gibbsite-kaolinite mixture with Sc concentrations >200 ppm. There, goethite is the main Sc carrier with up to 800 ppm Sc. Therefore, despite their relatively limited volumes, amphibolite-derived saprolites may also represent attractive targets for Sc in New Caledonia.

1 Introduction

Scandium (Sc), the 21st element of the periodic table, has several remarkable applications for the modern industry. The addition of small (<1 wt%) amounts of scandium to aluminium outstandingly increases its weldability and its resistance to stress, corrosion and heat, while maintaining light weight (Royset and Ryum, 2005; Toropova et al., 1998). Sc is therefore mainly used as hardening additive to aluminium to form Al-Sc alloys, with current applications ranging from the aerospace industry to the manufacture of high-quality sports equipment. In addition, scandium finds promising application in the development of Solid Oxide Fuel Cells (SOFCs), wherein the substitution of yttrium by scandium improves conductivity and lowers the operating temperature, extending fuel cell life. Also, Sc is notably used in high temperature lights, lasers and ceramics manufacturing.

Owing to its ionic radius and behavioral properties, Sc has historically been regarded as a heavy rare earth element. Sc, which exclusively occur in the +3 oxidation state, lacks affinity to combine with the common ore-forming anions. Thus, Sc^{3+} hardly concentrates through geological

processes and rarely forms Sc-rich minerals (Das et al., 1971; Emsley, 2014). Rather, it occurs as a trace element in a number of hydroxide, silicate, fluoride, sulfate and phosphate minerals. Consequently, although Sc is relatively common on Earth surface with an average crustal abundance of 22 ppm (Rudnick and Gao, 2014), it is only marginally produced (~15t/yr, US Geological Survey, 2016) and solely as a by-product of uranium, tungsten or bauxite ore processing, most exclusively in China and to a lesser extent in Kazakhstan, Russia and Ukraine. So far, the high quoted prices and the lack of organized market for scandium have prevented its widespread commercial adoption. However, increasing needs in energy saving technologies together with recent development of Sc extraction techniques have raised interest for this metal. In the last decade, Sc-rich occurrences with economically attractive grades and tonnages have been identified in some oxide-rich laterites developed after mafic and ultramafic rocks (Aiglsperger et al., 2016; Audet, 2008; Bailly et al., 2014; Chassé et al, 2017; Hoatson et al., 2011; Maulana et al., 2016; Ulrich, 2010). There, scandium enrichment is interpreted to be largely residual and resulting from the intense leaching of mobile cations during lateritisation of the parent rock, while scandium remains trapped and concentrated in neo-formed goethite. The initial Sc content of the parent rock is therefore of primary importance in controlling the Sc concentrations in its weathered derivatives. Two main types of Sc-bearing laterites are recognized, depending on the parent rock type. First, oxide-rich laterites developed after clinopyroxenites may yield Sc concentrations up to 300-600 ppm. To date, two high-grade (> 300 ppm) Sc lateritic camps, both located in New South Wales, Australia, have been identified and are under development for exploitation: the Syerston-Flemington-Owendale and the Nyngan camps. These laterites, considered as worldclass Sc deposits, are developed from alaskan-type clinopyroxenites which yield unusually high Sc concentrations of about ~100 ppm (Chassé et al., 2017). The lateritisation of these Sc-rich clinopyroxenites resulted in a threefold to sixfold increase of the Sc concentration, explaining the atypically elevated Sc grades (300-600 ppm) identified in their lateritic derivatives. Second, oxide-rich Ni-Co laterites developed after peridotites may yield Sc content up to 60-100 ppm, as observed in some Ni-Co laterites from

Queensland (Australia), New Caledonia, Philippines and the Cuba - Hispaniola islands of the Greater Antilles (Aiglsperger et al., 2016, Audet, 2008, Maulana et al., 2016; Hoatson et al., 2011). Previous investigations (Aiglsperger et al, 2016; Maulana et al., 2016; Audet, 2008; Ulrich, 2010) have shown that maximum Sc grades are observed in the goethite-dominated, yellow laterite horizon, representing about a tenfold enrichment compared to the parent peridotite, with higher Sc grades (100 ppm) being reached in harzburgite-derived laterites compared to dunite-derived laterites (60 ppm). Such concentrations are too low to be economically attractive as standalone Sc resources. Nevertheless, Sc could be a highly valuable by-product of Ni and Co processing, provided that (i) Sc-rich zones sufficiently overlap Ni- and/or Co-rich zones, and (ii) metallurgical plants allow low-cost extraction of Sc along with Ni-Co ore processing. Recently, several mining companies have developed industrialized plants for scandium recovery from Ni-Co laterites, demonstrating successful and cost-effective recovery of scandium from the hydrometallurgical extraction of lateritic Ni-Co ores. Among the primary producers of lateritic nickel and cobalt that may develop Sc co-beneficiation, opportunities exist for New Caledonia, as (i) its Ni (+Co) resources, accounting for about 11% of the world nickel resources, are dominantly hosted in oxide laterites, which are considered as the most favorable ore type for Sc co-valorisation, and (ii) the hydrometallurgical processing plant currently operated by Vale in the Goro mine (South Province) could allow operators to extract Sc directly on site. Additionally, some occurrences of weathered, amphibole-rich intrusive rocks have been recognised across the New Caledonian peridotite nappe (Cluzel et al., 2006). Such lithologies may host elevated amounts of Sc, close to that of the high-grade (300 ppm or higher) clinopyroxenite-derived laterites from the Syerston-Flemington and Nyngan deposits in Australia. In this contribution we examine the distribution of Sc in representative lateritic sequences of New Caledonia, accounting for the different types of protoliths and alteration styles. These include currently mined Ni-Co laterites developed after peridotites, wherein Sc may be a valuable by-product of Ni-Co production, as well as laterites developed after amphibole-rich, mafic intrusive bodies. Using a combination of field characterization, petrology, whole-rock and in situ major and trace element geochemistry

analysis, we address the major processes and the critical controls on the development of Sc-rich laterites in New Caledonia and discuss the potential for Sc valorization in New Caledonian laterites.

2 Regional geology

The New Caledonian archipelago, composed of several islands distributed along the Norfolk and Loyalty ridges in the South west Pacific, constitutes the emerged northern tip of the Zealandia continent, formerly part of the Gondwana supercontinent (Mortimer et al., 2017). The main island, referred to as "Grande Terre" (Figure 01), consists of a 300 km long allochtonous peridotite ophiolite tectonically overlying continental rock sequences of the Norfolk ridge (Cluzel et al., 2012a). The geological evolution of New Caledonia includes several tectonic phases. Importantly, the North-east-dipping subduction, which appeared to the East of New Caledonia at the Paleocene-Eocene boundary, ended during the Late Eocene with the obduction of the peridotite ophiolite after blocking of the subduction zone by the Norfolk Ridge at ca. 35 Ma (Cluzel et al., 2001, 2012a; Paquette and Cluzel, 2007). The peridotite ophiolite, which hosts the Ni-Co lateritic resources of New Caledonia, represents about 30% of the surface of Grande Terre. Exposed in the "Massif du Sud" southern unit and in several isolated tectonic klippes mainly aligned in the N140 direction along the west coast of the island (Koniambo, Tiebaghi, Poum massifs), the peridotite nappe is mostly composed of harzburgite locally interlayered with dunite, except in the northernmost klippes where lherzolite dominates (Ulrich et al. 2010). In the Massif du Sud, peridotites are locally overlain by layered pyroxenite and gabbro, representing the base of an oceanic crust (Guillon, 1975; Prinzhofer et al. 1980). The nappe does not exhibit any major internal thrusts and therefore did not experience thickening during its tectonic emplacement. Low temperature hydration of the oceanic mantle lithosphere resulted in the partial serpentinisation (20–60%) of the peridotite. In the main part of the nappe, serpentines principally occur as networks of mm-to ~10 cm-thick fractures and veins containing lizardite ± chrysotile. In contrast, the base of the peridotite nappe consists of a 20 to 200 m thick, subhorizontal, porphyroclastic and mylonitic serpentine sole formed during obduction, containing up to 100% serpentine (Avias,

1967; Orloff, 1968; Guillon, 1975; Cluzel et al., 2012a; Quesnel et al., 2013). Locally, amphibolite lenses occur at the base of the serpentine sole, above the Poya Basalt formation. These lenses are regarded as tectonic slices of the South Loyalty basin oceanic crust that recrystallized at ca. 56 Ma into the high-temperature amphibolite facies (Cluzel et al., 2012b). Also, ultramafic-mafic (amphibolite to micro-diorite), and felsic (leucodiorite to granite) coarse grain dykes are developed throughout the peridotite nappe, especially in the massif du Sud (Cluzel et al., 2006). These dykes, dated at ca. 53 Ma, are interpreted as slab melts and supra-subduction zone magmatic products. Subsequently, the emersion of New Caledonia during or soon after obduction lead to the development of a thick regolith cover that likely extended over the whole island. Several stepped planation surfaces were developed during repeated uplift phases and/or seas level changes until the Oligocene. In the northern part of Grande Terre, the laterite-blanketed peridotite has since been intensively eroded and dissected, so that it only remains as isolated klippes along the west coast of the island, whereas it is largely preserved in the southern lowlands and endorheic basins of the South Massif, where weathering probably continued until recently (Sevin et al., 2012, 2014). Some occurrences of pseudo-karstic structures in the peridotite nappe demonstrate the existence of an efficient drainage system (Genna et al., 2005; Trescases, 1975). Importantly, the extensive lateritisation of the peridotite ophiolite resulted in the formation of the worldclass lateritic Ni-Co resources mined in New Caledonia. Genetic models for Ni-Co laterites in New Caledonia involve (i) the leaching of most elements including Mg and Si after hydrolysis of olivine (0.4% Ni) and pyroxene (0.025% Ni), the redistribution and concentration of Ni within the saprolite by substituting Ni for Mg in secondary serpentines with up to 5% Ni and in garnierite veins, which can grade over 20% Ni, and (iii) the development of Ni-bearing oxide-rich (lateritic) horizons at the expense of the saprolite (Butt and Cluzel, 2013; Cathelineau et al., 2016, 2017; Freyssinet et al., 2005; Golightly, 2010; Manceau et al., 2000; Trescases, 1975; Wells et al., 2009). The Ni-rich, silicate ± garnieritic ore has been actively mined since the late 19th century but reserves are rapidly being depleted. The overlying lateritic ore yields lower Ni concentrations (1.0–1.5% Ni). However, laterite ore reserves are enormous and will represent the bulk of Ni

reserves of New Caledonia in the future. Also, Ni laterite ores often yield elevated (>2000 ppm) cobalt concentrations adding significant value to the ore. Currently, co-extraction of Ni and Co from oxide laterite ore is successfully applied at the Goro processing plant (Massif du Sud). Similarly, Sc may add significant value to lateritic Ni(-Co) ore as it is assumed to be concentrated in the yellow laterite horizon. Although lateritic profiles in New Caledonia mostly consist of a saprolitic zone with mixed hydrous silicates and oxides that directly grades upwards into a lateritic zone essentially composed of oxides and oxyhydroxides, a few lateritic profiles exhibit well-developed, Ni-rich smectitic zones below the lateritic zone. The development and preservation of Ni smectitic ore, mostly observed in Tiebaghi Ni-laterites and more locally in some low-altitude laterites of the Boulinda massif (Latham, 1986; Trescasses, 1975), probably relates to relatively lower drainage conditions during weathering. As suggested by previous studies documenting the distribution of Sc in some dunite- and harzburgite-derived Ni laterites from New Caledonia, both the type of peridotite protolith and the styles of lateritic alteration are important parameters controlling the maximum Sc grades (Audet, 2008; Bailly et al., 2014). So far, no data is available on Sc in lherzolite-derived Ni-laterites, although Ulrich (2010) observed Sc content up to 20 ppm in some unweathered lherzolites. Differences in the Sc content of peridotites likely relate to their variable proportions of magnesian olivine (forsterite), orthopyroxene (enstatite) and clinopyroxene (diopside). With regards to the mafic intrusive rocks documented by Cluzel et al. (2006), no data on Sc is available neither on the unweathered lithologies nor in their lateritic derivatives. In the following, we document and discuss the distribution of Sc in some representative mafic and ultramafic-derived lateritic profiles of New Caledonia.

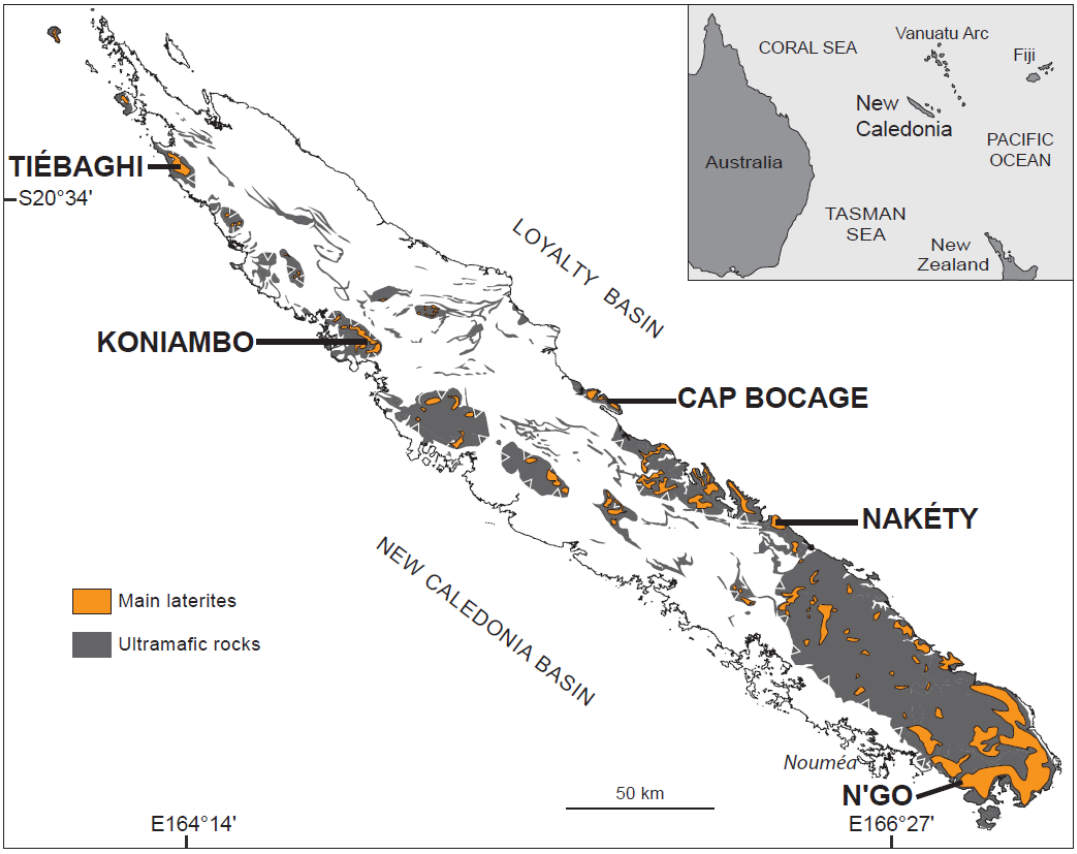

Figure 01: Geology map of New Caledonia. Modified from Maurizot and Vendée-Leclerc (2009).

3 Methodology

3.1 Sampling strategy

In order to investigate the scandium distribution in representative laterites from New Caledonia, sampling strategy has been accordingly developed to encompass the diversity of peridotitic (harzburgite, dunite, lherzolite ± serpentinite) and mafic to ultramafic intrusive (gabbro, pyroxenite, amphibolite) protholiths. Selected Ni-laterites include (i) six harzburgite-derived laterites from Koniambo, N'Go, Nakéty and Cap Bocage, (ii) two dunite-derived laterite from Cap Bocage and N'Go, and (iii) two lherzolite-derived, atypical clay-rich laterites from Tiébaghi (Figure 01). Selected lateritic profiles are mostly preserved from erosion and were sampled from the bedrock to the ferricrete. Sampling was mainly conducted on 15 to >60m deep diamond drill holes that penetrates the near-surface weathering down to the bedrock. Holes were logged in terms of their rock types, alteration styles and alteration intensity. Drill hole sampling was twinned with

field observations in corresponding open pits when accessible. Complementary sample collection has been conducted along open pit walls for some key facies and profiles when accessible/necessary (i.e. no drill holes available). Also, five amphibolite or amphibole-bearing pyroxenite dykes and their lateritic derivatives were sampled in N'Go and Nakéty, together with two profiles of lateritised gabbro dykes and their peridotite-derived laterite hosts in Koniambo and N'Go. Eventually, discrete samples of pristine amphibolitic gabbros were collected in N'Go, Nakéty and Tiébaghi. Location coordinates are given using the RGNC Lambert NC geographic coordinate system.

3.2 Analytical strategy

Sixty polished thin-sections were prepared from collected samples and examined using reflected/transmitted light and scanning electron microscopy with a JEOL JSM7600F at the Georessources Laboratory and at the SCMEM. In situ mineral chemistry analysis for major elements (Na, Mg, Al, Si, P, Ca, Ti, Mn, Fe, Co, Ni) was conducted on electron microprobe (EPMA, WDS analysis) Cameca SX100 at the SCMEM with typical voltage intensity of 15kV and 10nA, respectively. In situ analysis for Sc and other trace elements was conducted using either electron microprobe or LA-ICP-MS. Specific conditions for electron microprobe WDS analysis of Sc are 25kV and 150nA, with both detection limit and accuracy of about 50 ppm. LA-ICP-MS analysis of Sc in silicates was performed with the NIST60 standard. For oxides, in-house standards were developed and validated (Ulrich et al., in prep.). Detection limit is below 2 ppm for most trace elements. Ablation time and spot sizes are 45 s and 60 microns, respectively. Data processing was conducted using the Sills program (Guillong et al., 2008).

Hand specimens were crushed using an agate bowl pulveriser at GeoRessources Laboratory, and pulps were analysed for whole-rock major- and trace-element geochemistry at the SARM analytical service of the CRPG. Major element oxides and Sc were analysed using ICP-OES iCap6500 with Li borate fusion. Trace elements were analysed by ICP-MS iCapQ with Li borate fusion followed by nitric acid digestion. The loss on ignition (LOI) component was determined by

drying sample powders overnight at 110C, ignition at 1100C and subsequent measurement of the weight loss. Analytical accuracy (2s standard deviation) lies within typical uncertainty of the analytical data for both major oxides and trace elements, that is less than 1% for major oxides and less than 5% for most trace elements.

4 Geology of investigated sites

4.1 Ni-Co-laterites developed after peridotites

In the five investigated districts (Figure 1), Ni-Co laterites exhibit a suite of alteration facies with specific mineral assemblages and composition. All the Ni-Co laterites are developed after serpentinised peridotites of variable type. In Koniambo and Nakéty, harzburgite is predominant. In N'Go and Cap Bocage, harzburgite also dominates but it is interlayered with significant volumes of dunite. In Tiébaghi, lherzolite dominates over harzburgite, although the intensive serpentinisation of the peridotite complicates its univocal recognition in the field. The intensity of serpentinisation in unweathered peridotites is variable and relates, at the district- to regional-scale, to the vertical proximity of the peridotite with the serpentine sole developed at the base of the ophiolite nappe (positioned at ca. 200m in elevation). Tiébaghi Ni-Co laterites, located at low altitude (200-400m), are therefore developed after intensely serpentinised peridotites. In contrast, in Ni-Co laterites developed at higher altitude (e.g. Koniambo massif laterites positioned at 900m, i.e. well above the serpentine sole), serpentinisation mostly occurs as mm to dm-large veins of serpentine distributed as fracture networks within the peridotite (Figure 02A).

Saprolitisation of the peridotite initiates along fractures, often using pre-existing structures, and progresses pervasively from these fractures into the fresh peridotite boulders. There, hydrolysis of olivine and pyroxene results into an increase of porosity while largely maintaining hardness. Diffuse greenish coloration of the rocky saprolite likely relates to an increase of the Ni content (Figure 2D). Also, veins of high grade, greenish talc-like (kerolite) are best expressed in the rocky saprolite and root into the fresh peridotite (figure 2B). Rocky saprolite is usually poorly developed in thickness (< 50cm) and sharply evolves upwards into earthy saprolite (e.g. in the OPB7 profile,

Koniambo, Figure 3A) wherein the total silicate content drops below 20% after hydrolysis of most of the remaining silicates (Figure 2C, 2D, 3A). In some other profiles, rocky saprolite may be thicker (~3m) and remains partly preserved as hard cores within the overlying earthy saprolite (e.g. in the PZ1B profile, cap Bocage, figure 3A). Although earthy saprolitic material is friable, primary structures remain essentially preserved with minimal compaction, further increasing the porosity so that the bulk density of dry earthy saprolite may drop below 1 (referred to as "minerais bouchon" or "cork ore" by local miners for its buoyancy properties). Noteworthily, some atypical lateritic profiles exhibit well developed Ni smectite-rich zones below the oxide-rich zone (Figure 2E, 3A). Such laterites are mostly developed in the northernmost klippes and particularly at Tiébaghi (Fantoche, East and South Alpha deposits). Also, similar extensive occurrences of Ni-smectites were recognized during our investigations in the Ma-oui deposit of the Koniambo mine.

The interface between the earthy saprolite and the overlying laterite, referred to as the transition laterite, is marked by the progressive disappearance of primary structures and the subsequent compaction of the earthy saprolite. The transition laterite often exhibits significant concentrations of Mn-Co-Ni oxides (lithiophorite, asbolane) either as mm- to cm-thick veins or as diffuse accumulation in the iron-rich matrix (Figure 2F, 3A). The transition laterite evolves upwards into the usually well-developed yellow laterite wherein goethite (limonite) predominates. The yellow laterite then grades into the red laterite wherein hematite forms at the expense of goethite resulting in a mineral assemblage dominated by goethite and hematite. Eventually, lateritic profiles are capped by massive to vesicular ferricrete and pisolithic horizons. These uppermost units are largely dissected and dismantled by erosion so that boulders of the ferruginous hardcaps often appear encapsulated in the underlying loose lateritic material (Figure 2G, 2H, 3A).

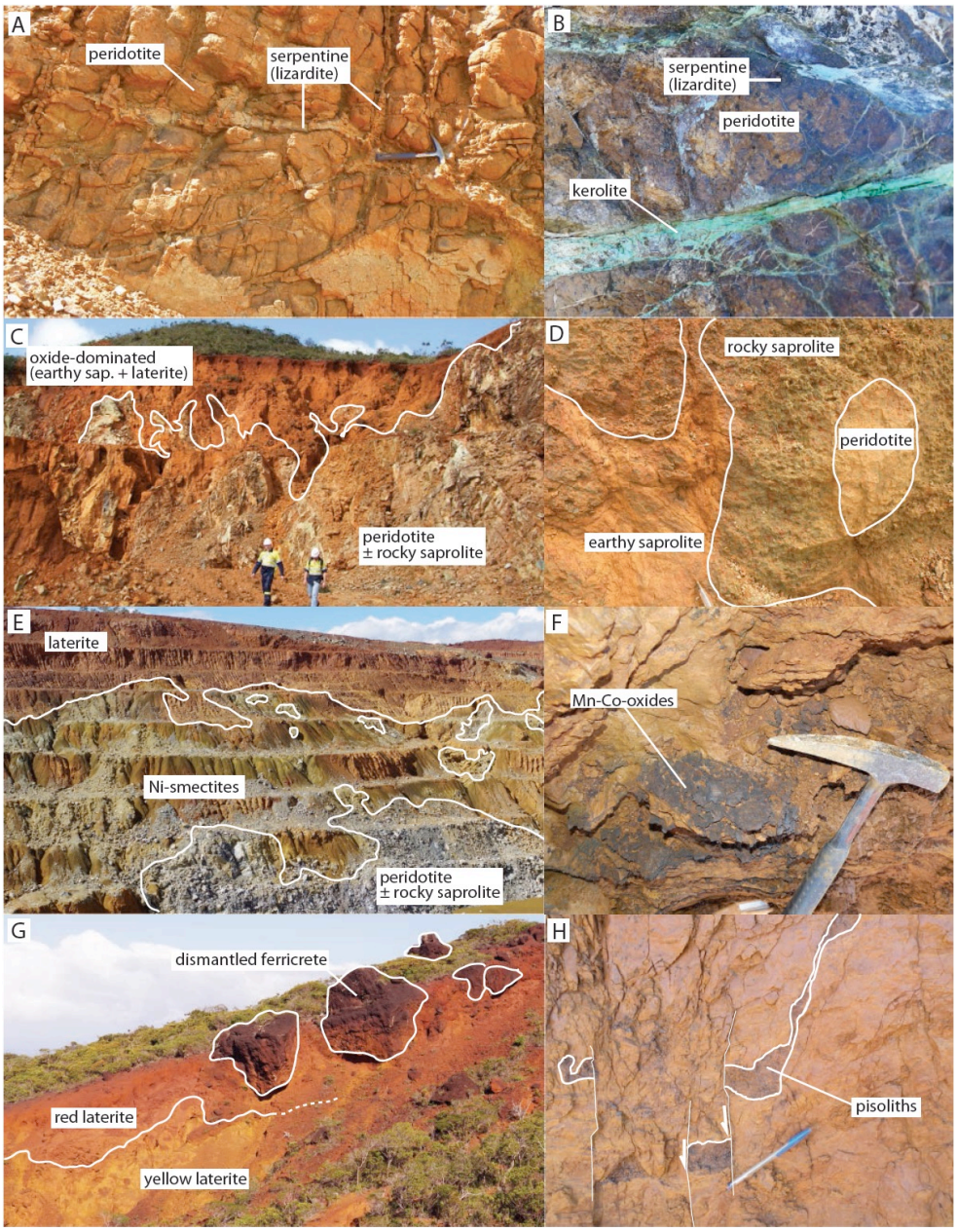

Figure 2: Field photographs of peridotite-derived laterites. (A) Unweathered harzburgite with networks of serpentine (lizardite) veins (Koniambo), (B) Ni-rich talc-like (kérolite) vein developed at the bedrock – rocky saprolite interface (Koniambo), (C) Typical sharp transition from silicate-dominated bedrock and rocky saprolite to oxide-dominate earthy saprolite and laterite (Koniambo). (D) Altered boulder of peridotite grading outwards from unweathered dunite to rocky and earthy saprolite. The rocky saprolite is poorly developed (<20 cm in thickness) and readily grades into oxide-dominated earthy saprolite (Cap Bocage). (E) Well-developed Ni smectite-rich zone (up to >15m in vertical thickness) above lherzolitic serpentinite

at Tiébaghi. (F) Mn-Co oxide-rich transition laterite developed at the earthy saprolite – yellow laterite interface (Cap Bocage). (G) Yellow laterite grading upwards into red laterite. The red laterite encapsulates boulders of the dismantled ferricrete (Tiébaghi). (H) Neptunian dyke of pisolithic material into the yellow laterite (Cap Bocage).

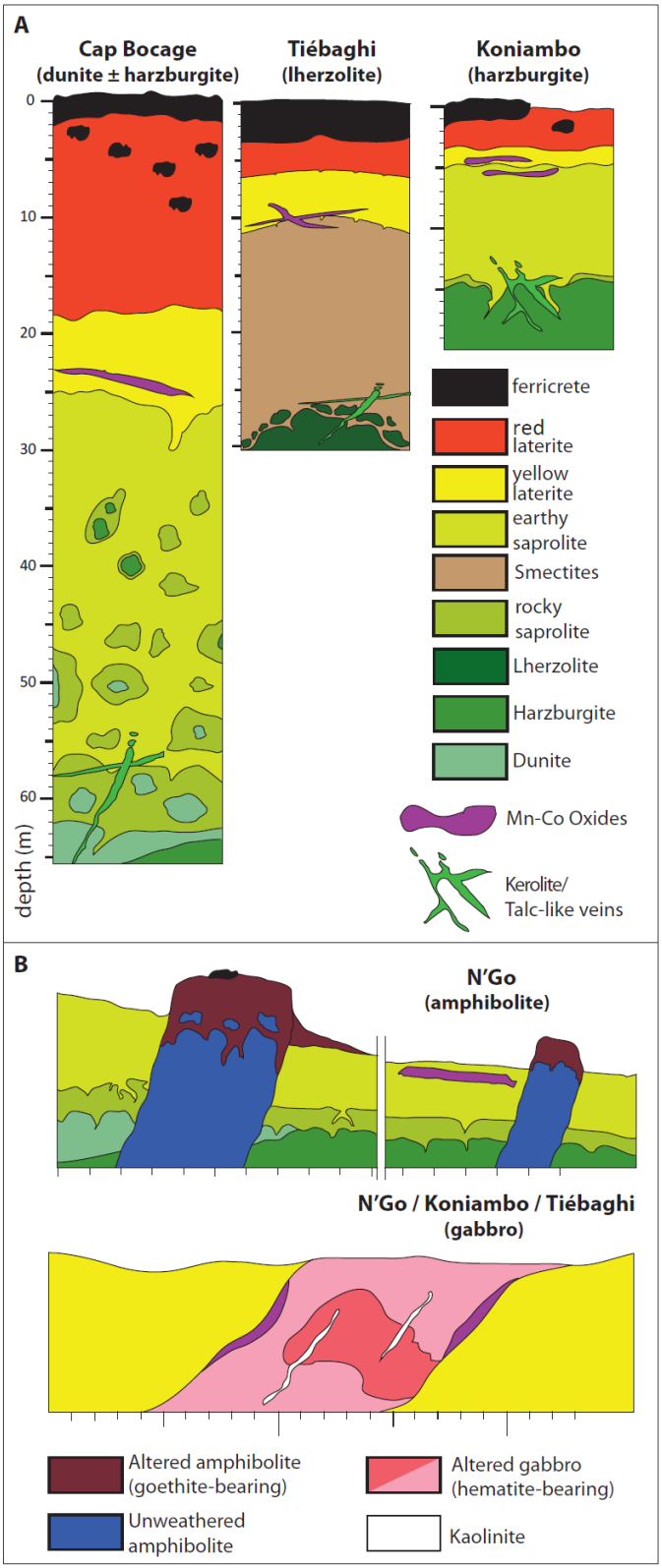

Figure 3: Stratigraphic logs and cross sections of representative laterites (A) Peridotite-derived laterites. (B) Amphibolite- and gabbro-derived laterites.

4.2 Laterites developed after mafic-ultramafic intrusive rocks

The mafic dykes identified in N'Go, Nakéty and Tiébaghi display a suite of texture and mineralogy. Amphibolite and amphibolitic pyroxenite exposed in N'Go and Nakéty occur as subvertical dykes, locally forming swarms, with thickness ranging from <10 cm up to >10 m (Figure 3B, 4A). Amphibolites and amphibole-bearing pyroxenites are commonly more resistant to weathering than the surrounding peridotites, and therefore form positive relief in outcrops (Figure 4A). These dykes contain variable proportion of amphibole and pyroxene, from amphibolitic pyroxenites where pyroxene dominates to amphibolites essentially composed of amphibole, and variable crystal size, from fine-grained (pyroxene and amphibole <1mm) to pegmatitic (amphibole up to 10 cm, pyroxene up to 5 mm) textures. Such variability is observed down to the outcrop scale, where two adjacent dykes often display marked differences in thickness, texture and/or composition. Noteworthily, one large (> 10 m in thickness) intrusive body identified at N'Go shows internal zonation of texture and mineralogy, from zones consisting of monomineralic amphibolite to zones dominated by pyroxene with giant (>10 cm) amphibole porphyroblasts (Figure 4E). Similarly, dykes of amphibolitic gabbros identified in Tiébaghi, N'Go, Nakéty (Figure 4F) display variable crystal size, from fine grained to pegmatitic texture, and contain variable proportion of feldspar (~50 to 90 vol%) and amphibole (~10 to 50 vol%).

Due to their increased resistance to weathering, amphibolites and amphibole-bearing pyroxenites exposed in outcrops exhibit alteration that generally penetrates only to shallow depth (few cm to few m) below surface, contrasting with the well-developed laterite profiles derived from peridotites (15 to 60 m in thickness). The most evolved alteration product of these dykes consists of brownish, goethite-bearing earthy saprolitic material, wherein primary silicates have been largely leached away although primary structures remain preserved. Stricto sensu laterites, i.e. with obliterated textures, are rarely observed. Owing to the positive relief formed by these dykes relative to the surrounding peridotite-derived laterites, fragments of amphibolite- or pyroxenite-derived earthy saprolite may accumulate downslope in outcrops (Figure 4A). Comparatively, amphibolite-bearing gabbros are more readily altered as they mainly contain weatherable

feldspar, so that they may alter to greater depth and form friable lateritic material (Figure 4B). Importantly, whereas amphibolite and pyroxenite usually alter to form brownish, goethite-bearing saprolite, gabbro alters to pinkish, hematite- and kaolinite-bearing saprolite/laterite (Figure 4B). Color zonation patterns are commonly observed in weathered gabbros, from whitish or pale pinkish facies dominated by kaolinite to cherry pinkish facies with higher proportions of hematite (Figure 4D). Such zonation likely results either from primary zonation in the gabbro or secondary segregation of Fe and Al during weathering. As discussed below, the observed discrepancy in the nature of secondary iron-bearing phases (goethite vs. hematite) formed through weathering of mafic-ultramafic dykes (amphibolite and pyroxenite vs. gabbro) is of major importance in controlling Sc distribution in their weathered derivatives.

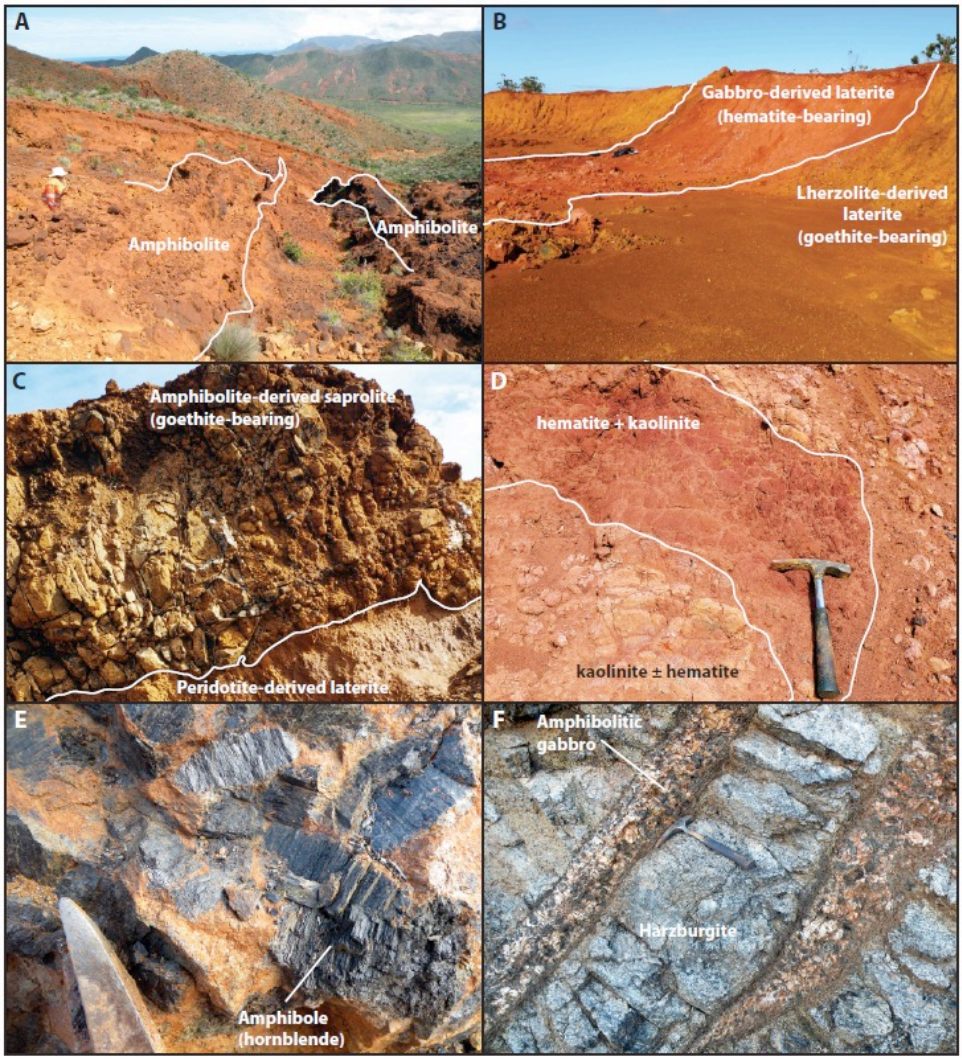

Figure 4: Field photographs of amphibolite- and gabbro-derived laterites. (A) Weathered amphibolite dykes cutting across harzburgite-derived laterite. Exposed dykes form positive reliefs due to increased resistance to weathering (N'Go), (B) Hematite-bearing, gabbro-derived laterite cutting across lherzolite-derived laterite (Tiébaghi). (C) Goethite-bearing, saprolitised dyke of amphibolite overlying harzburgite- or dunite-derived laterite (N'Go), (D) Internal facies zonation within gabbro-derived saprolite exhibiting pale reddish zones dominated by kaolinite ± hematite and darker reddish zones with higher proportions of hematite (Tiébaghi), (E) Unweathered amphibolite containing amphibole (hornblende) megacrystals (N'Go), (F) Unweathered amphibole-bearing gabbro intrusions (Tiébaghi).

5 Scandium in parent rocks

5.1 Peridotites

5.1.1 Mineral assemblages

Unweathered peridotites exhibit typical mineral assemblages essentially including (i) primary (mantellic) magnesian olivine (forsterite), orthopyroxene (enstatite) and clinopyroxene (diopside), whose relative proportions depend on the type of peridotite, and (ii) secondary (developed at the expense of mantellic silicates) serpentine (mainly lizardite), whose relative proportion depend on the degree of serpentinisation. In dunite, as observed in N'Go and Cap Bocage, forsterite is the predominant (> 90 vol%) mantellic silicate (Figure 5A-5C) while enstatite may only be present as an accessory phase, both mineral forming automorph crystals up to ~8mm. Accessory chromiferous spinel also occurs as a late-crystallizing, interstitial phase (Figure 5C). Comparatively, harzburgite exhibits higher proportion of enstatite (>10 vol% and up to ~30 vol%) at the expense of forsterite. Noteworthily, some harzburgites identified at Koniambo and Nakéty contain diopside as accessory phase (<1 vol%), either overgrowing enstatite crystals or as a late interstitial phase. In lherzolite, proportions of enstatite and forsterite are about 45 vol% while the diopside content increases up to 5-10 vol% forming large, automorph crystals, as well as exsolutions within enstatite. Secondary serpentinisation, characterized by the formation of

lizardite ± chrysotile at the expense of primary mantellic silicates, is ubiquitous within the peridotite. In moderately (~30-50%) serpentinised peridotites (i.e. distal to the serpentine sole), lizardite occur mainly as vein network (or mesh) fragmenting olivine and pyroxene crystals (Figure 5A-5I). Pervasive serpentinisation of the fragmented silicates may be observed but rarely penetrates deep into the primary silicate crystals. In strongly serpentinised peridotites, such as the lherzolite-derived serpentinites typically observed in Tiébaghi, most if not all the primary silicates are pseudomorphologically replaced by lizardite after extensive, pervasive serpentinisation (Figure 5J-5K). Serpentinisation is commonly accompanied by the formation of magnetite, either along initial crystallographic planes of serpentinised enstatite or as euhedral crystals in serpentinised forsterite (Figure 5K-5L). Also, some calcite veins developed at the expense of diopside are locally observed in moderately serpentinised lherzolites (Figure 5H). These veins, which are not recognized in highly serpentinised peridotites, probably formed early during the serpentinisation process and were subsequently replaced by lizardite after complete serpentinisation of the peridotite.

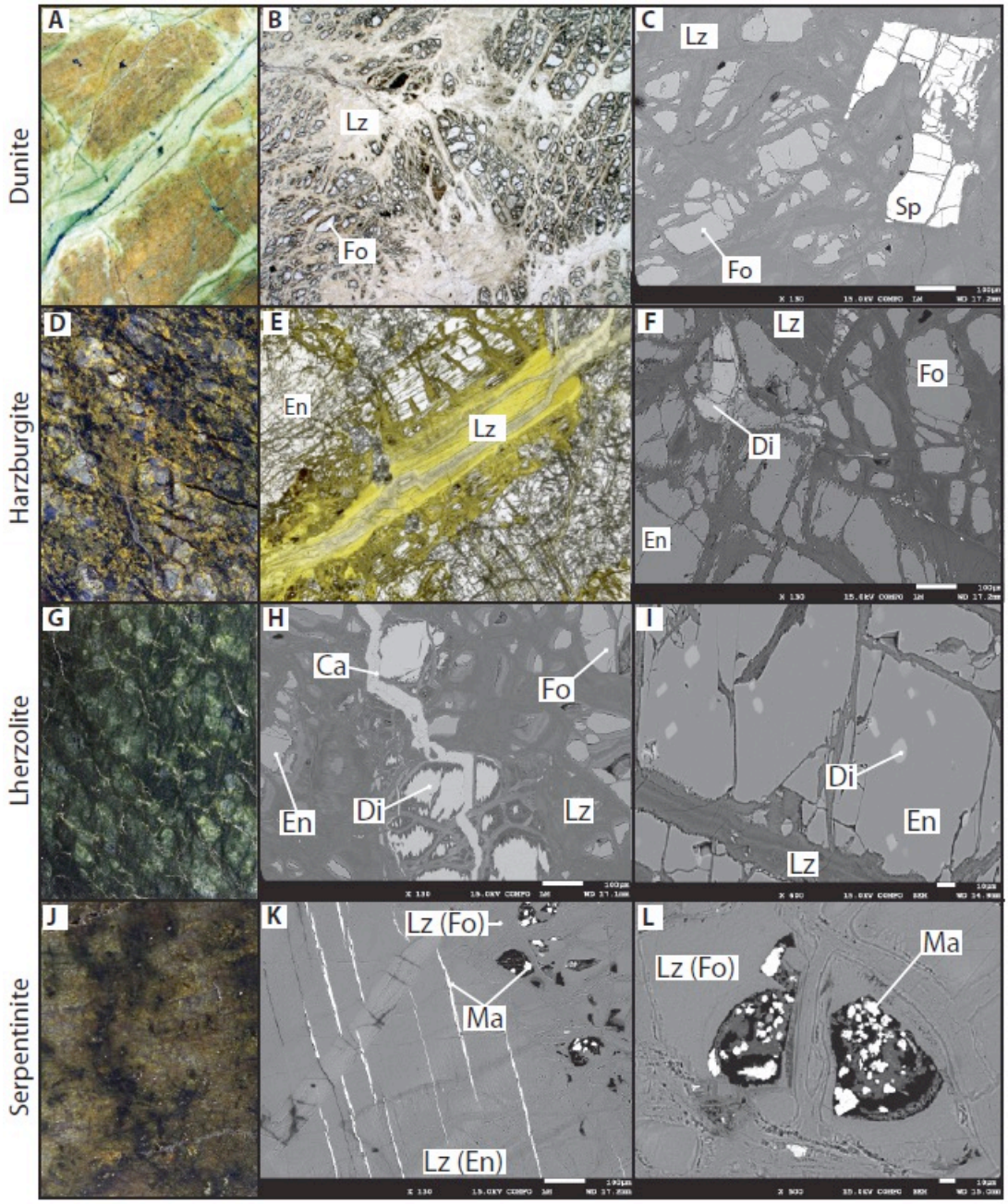

Figure 5: Optic and SEM microphotographs of mineral assemblages in peridotitic bedrocks. (A-C) Dunite from Cap Bocage, (D-F) Harzburgite from Koniambo, (G-I) Lherzolite from Tiebaghi, (J-K) serpentinite from Tiébaghi. Mineral abbrev.: Lz = lizardite, Fo = forsterite, Sp = spinel, En = enstatite, Di = diopside, Ca = calcite, Lz(Fo) = lizardite after forsterite, Lz(En) = lizardite after enstatite, Ma = magnetite.

5.1.2 Major and trace element geochemistry

Eleven samples of unweathered peridotites including dunite, harzburgite, lherzolite and lherzolite-derived serpentinite were analysed for whole-rock major and trace element geochemistry (Table 1). Also, six samples of unweathered lherzolite from the Babouillat zone of the Tiébaghi massif analysed by Ulrich (2010) were included to this dataset. Si, Mg and to lesser extent Fe are the principal constitutive elements in peridotites, with SiO_2, MgO and FeO concentrations of 38-43, 35-45 and 6-7 wt%, respectively (Figure 6A). Whole-rock concentrations for major elements are consistent with the mineral chemistry of the principal constitutive phases (forsterite, lizardite, enstatite) as analyzed by EPMA (Figure 6A). Moderately serpentinised dunite and harzburgite yield the highest MgO content owing to higher proportion of Mg-rich forsterite. The elevated LOI illustrates the significant contribution of hydrous serpentine (lizardite) in peridotites, from about 6 wt% LOI in moderately serpentinised (~30% serpentine) peridotites to about 17% in serpentinites (~100% serpentine). Al_2O_3 and CaO concentrations vary from about ~0.25 wt% in dunite to about 2 wt% in lherzolite (Figure 6A) and are therefore inversely correlated with MgO. The Al_2O_3 content of peridotites mostly relates to the proportion of Al-bearing (1.6 to 3 wt% Al_2O_3) enstatite (Figure 6A). The CaO content also largely relates to the proportion of enstatite although accessory, Ca-rich diopside (~24 wt% CaO) may significantly contribute to the total CaO content of lherzolites. The Cr_2O_3 content of peridotites ranges from 0.3 to 0.5 wt% and results from the contribution of enstatite and accessory Cr-spinel. The Ni content ranges from 0.20 to 0.25 wt% with higher grades reached in harzburgite and dunite owing to higher proportion of Ni-bearing forsterite (0.25-0.40 wt% Ni).

Similar to Al, Sc exhibits large variations of concentration in peridotites, from 3-5 ppm in dunite to 6-8 ppm in harzburgite and 10-25 ppm in lherzolite (Figure 6B). Noteworthily, lherzolites investigated in this study from the Alpha and Fantoche deposits (Tiébaghi) have relatively low Sc concentrations (~10 ppm) whereas lherzolites from the Babouillat zone (Tiébaghi) analysed by Ulrich (2010) yield higher Sc concentrations (15-25 ppm). LA-ICP-MS analysis (Figure 7) indicates that the Sc content in mantellic silicates increases from forsterite (3-7 ppm) to enstatite (15-30 ppm) and diopside (40-70 ppm), so that the increase of the Sc content in peridotites from dunite

to harzburgite and lherzolite relates to increasing proportions of enstatite (and accessorily diopside) at the expense of forsterite. The Sc content of enstatite and diopside may vary depending on the considered peridotite massif. Enstatite in dunite and harzburgite from the N'Go massif yields Sc content of 15-20 ppm, while enstatite in harzburgite from the Nakéty and Koniambo massifs yields Sc content of 20-30 ppm, and enstatite in lherzolite from the Tiébaghi massif yields Sc content of ~30 ppm. Similarly, diopside in harzburgite from Koniambo yields Sc content of 40-50 ppm while diopside in harzburgite from Nakéty and in lherzolite from Tiébaghi yields Sc content of 60-70 ppm (Figure 7). Sc concentrations in lizardite (5-50 ppm) strongly depend on the Sc content of the mantellic silicate precursors and therefore cover most of the range observed in primary silicates (Figure 7). It is assumed that the degree of serpentinisation does not affect the whole-rock Sc content of peridotites.

Noteworthily, whole-rock Sc concentrations are well correlated with V and to a lesser extent with Al concentrations (Figure 6B), so that the whole-rock Sc content of peridotites may be approximatively estimated from the Al and V concentrations as following:

(1) $Sc\ (ppm) = 10.6 * Al_2O_3\ (wt\%) = 0.23 * V\ (ppm)$

These whole-rock correlations result from the co-increase of the Sc, V and Al content from forsterite to enstatite and diopside (Figure 7). In enstatite, Sc and Al concentrations define a trend from low-Al-Sc enstatite in N'Go and Cap Bocage dunite and harzburgite (3000-5000 ppm Al, 10-20 ppm Sc) to higher-Al-Sc-enstatite in Tiébaghi lherzolite (15000-20000 ppm Al, ~30 ppm Sc) with intermediate concentrations occurring in enstatite from Nakéty and Koniambo harzburgites. The co-increase of Al and Sc in peridotites is therefore not only due to increasing proportions of enstatite at the expense of forsterite, but also to increasing Al and Sc concentrations within enstatite from dunite and harzburgite facies of the southern massifs to harzburgite and lherzolite facies of the northern massifs. In Sc-rich lherzolite (>15 ppm), enstatite alone can hardly account for the elevated Sc content. In such facies, diopside contributes significantly to the whole-rock Sc budget. Also, mineral chemistry data indicates that Sc and V concentrations co-increase from

forsterite to enstatite and diopside, so that the Sc content of peridotitic mineral phases may be approximatively estimated from its V content as following:

(2) $Sc\ (ppm) = 0.26*V\ (ppm) + 6$

Increasing proportions of Sc- and V-bearing enstatite and diopside in peridotites well explain the Sc–V correlation identified from whole-rock analysis (Figure 6, 7). Eventually, Sc and Ti concentrations in primary silicates may exhibit correlation trends from low-Sc-Ti-forsterite to higher-Sc-Ti-enstatite and diopside. However, contrasting with Sc-Al and Sc-V correlation trends, Sc-Ti correlation trends display specific slopes depending on the considered peridotite massif, suggesting that Sc-Ti correlations may only be defined at the massif scale.

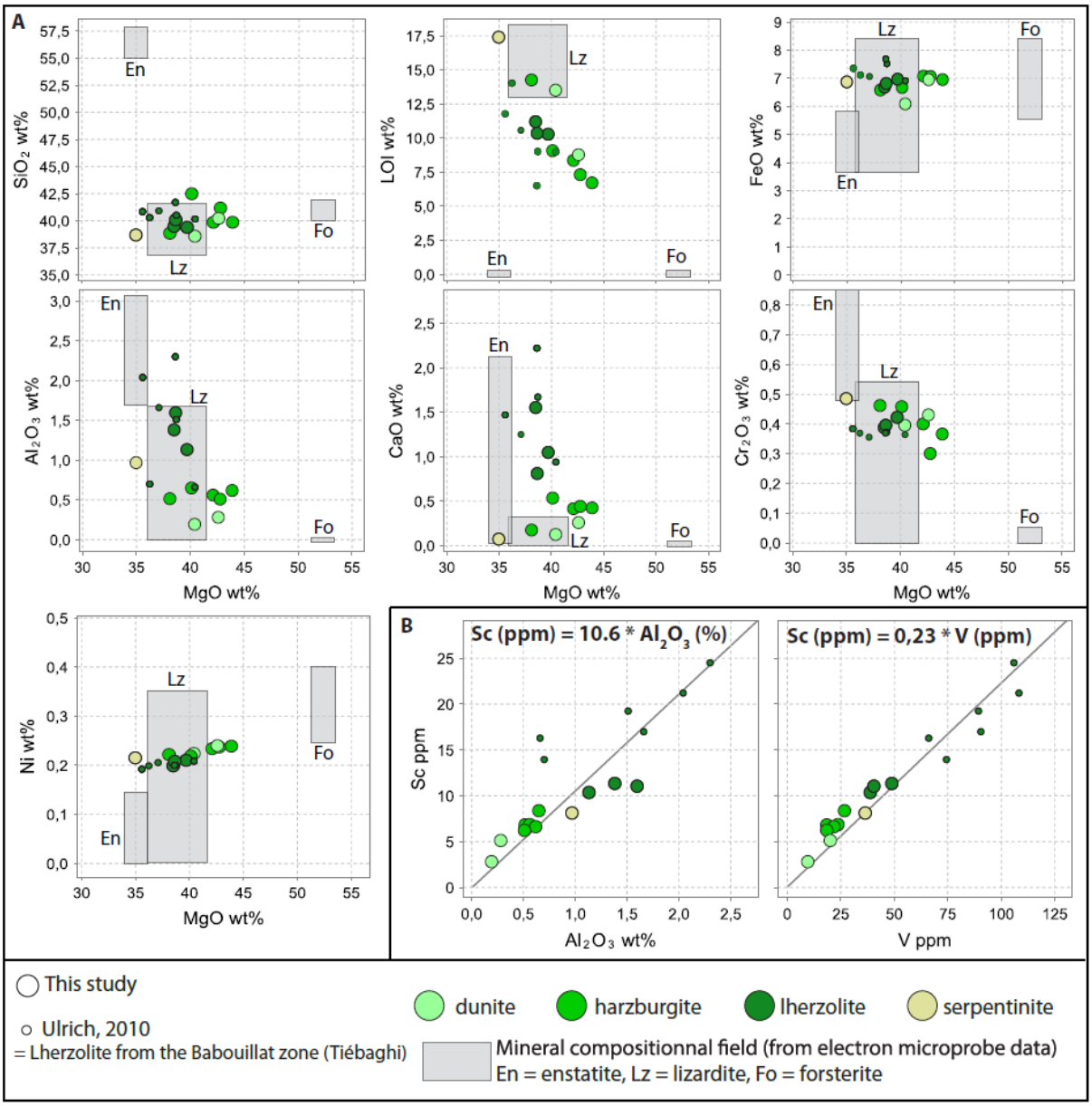

Figure 6: Whole-rock geochemistry data for peridotites (dunite, harzburgite, lherzolite and serpentinite). (A) Plots of SiO_2, LOI, FeO, Al_2O_3, CaO, Cr_2O_3 and Ni (wt%) against MgO (wt%). Grey rectangles indicate mineral compositions from electron microprobe data. (B) Plots and correlations of Sc (ppm) against Al_2O_3 (wt%) and V (ppm).

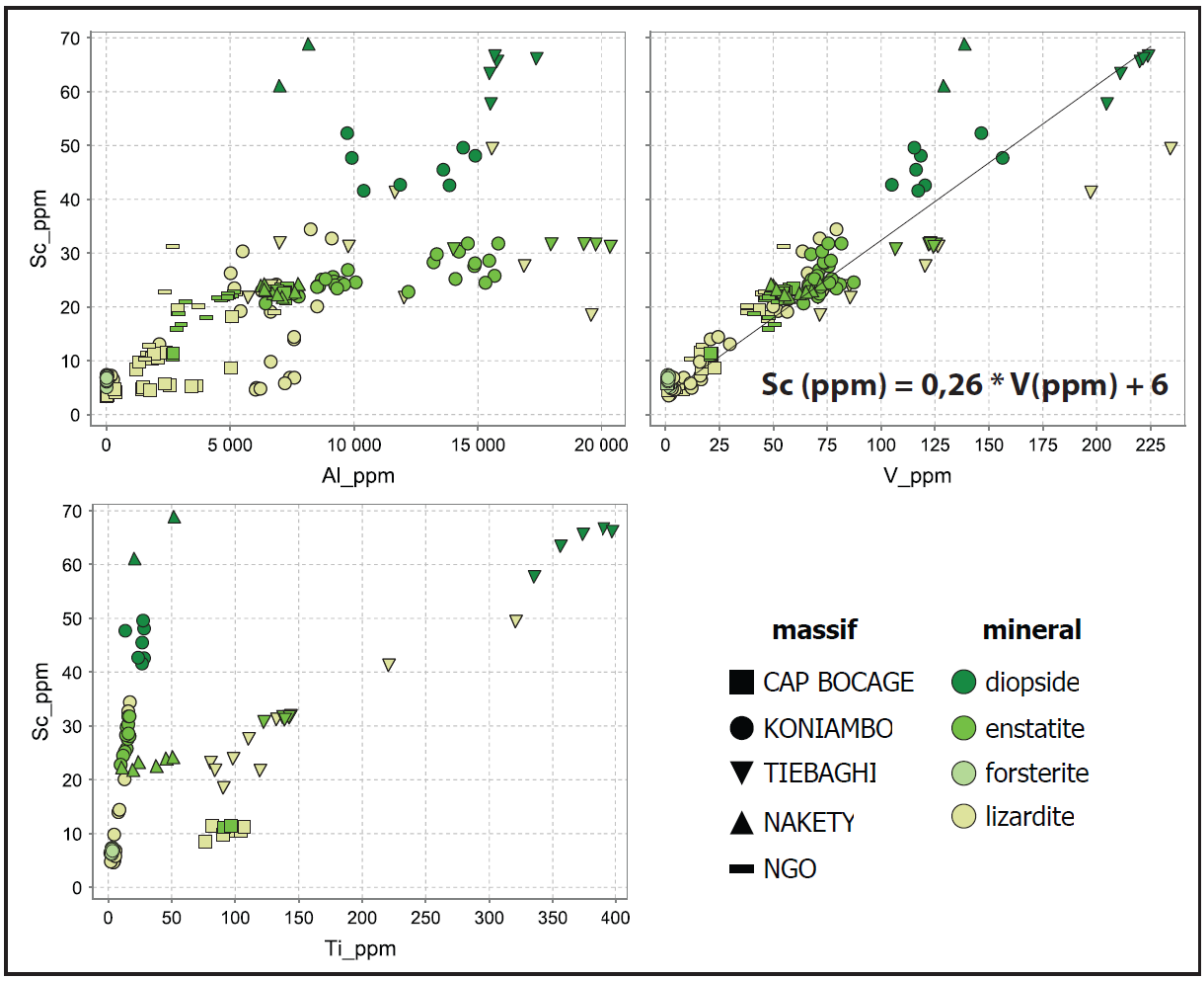

Figure 7: Plots and correlations of Sc (ppm) against Al, V and Ti (ppm) in peridotitic minerals (diopside, enstatite, forsterite and lizardite) from LA-ICP-MS data.

5.2 Mafic-ultramafic intrusive rocks

5.2.1 Mineral assemblages

Unweathered mafic-ultramafic intrusive rocks including amphibolite, amphibolitic pyroxenite and amphibolitic gabbro exhibit specific mineral assemblages and textures. Amphibolite occurrences identified in Nakéty and N'Go contain over 90 vol% hornblende with crystal size ranging from <500 µm to ~10 cm together with minor enstatite and accessory titanite and Fe-Ti-oxides (Figure 8A-8C). Textural relationships indicate that hornblende develops surrounding corroded enstatite cores. Similar mineral assemblages are observed in amphibolitic pyroxenite although enstatite occurs in greater proportion from >10 up to 80 vol% (Figure 8C-8E). Whereas hornblende may develop porphyroblastic textures with crystals up to 10 cm, enstatite crystal size

rarely exceeds 5 mm. Amphibolitic gabbro and microgabbro from N'Go, Nakéty and Tiébaghi contain 50 to 90 vol% plagioclase and 10 to 50 vol% hornblende, together with accessory Fe-Ti oxides, sulfides and/or phosphates (Figure 8G-8L). As confirmed by mineral chemistry analysis (see below), plagioclase exhibit various composition ranging from anorthite to andesine. In all mafic-ultramafic dykes, secondary chlorite commonly forms at the expense of enstatite and plagioclase (Figure 8L). Prehnitisation of anorthite is also observed in some gabbro occurrences from Tiébaghi.

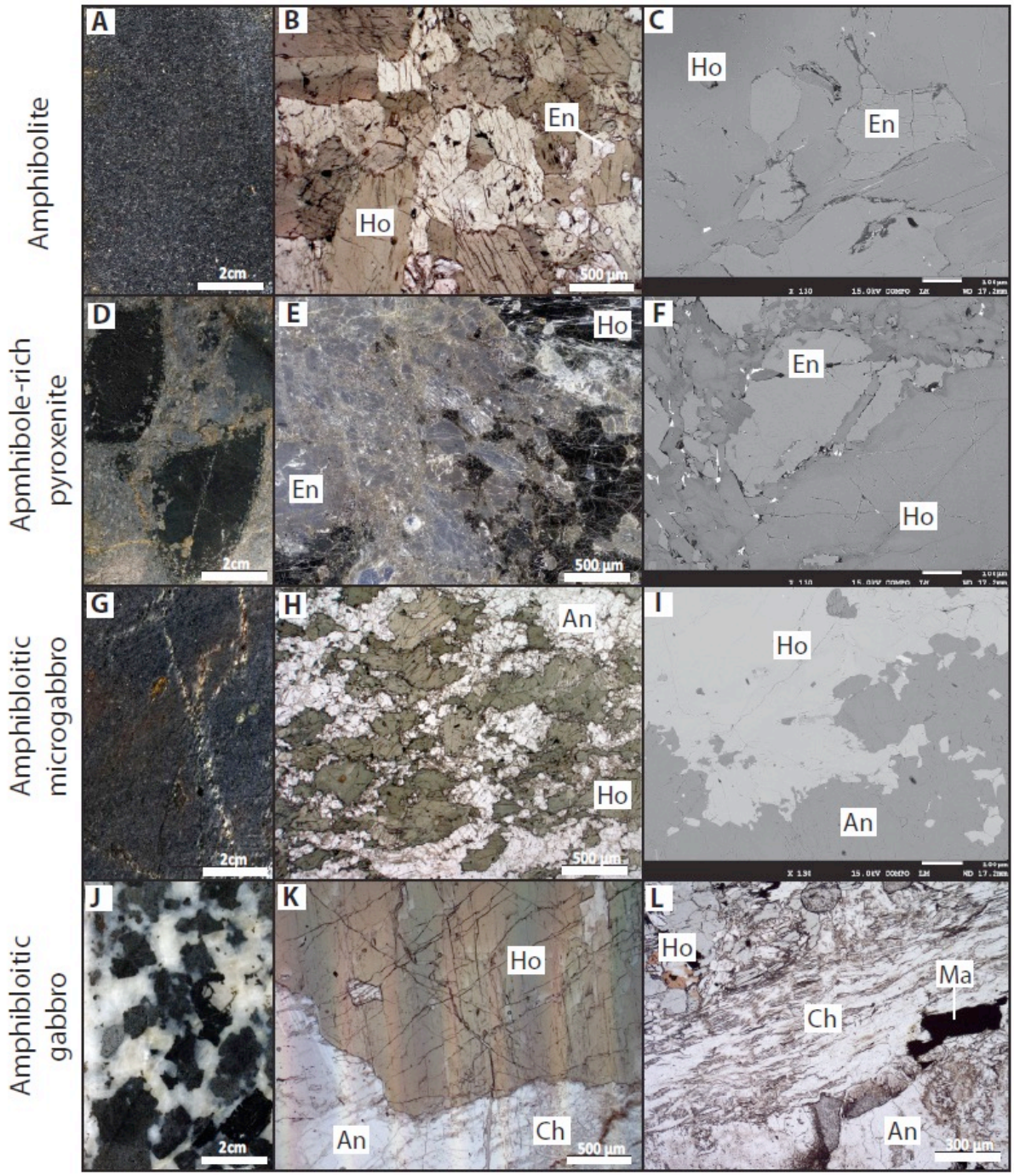

Figure 8: Optic and SEM microphotographs of mineral assemblages in mafic intrusive bedrocks from N'Go, Nakéty and Tiébaghi. (A-C) Amphibolite, (D-F) Amphibole-bearing pyroxenite, (G-I) amphibolitic microgabbro, (J-K) amphibolitic gabbro. Mineral abbrev.: Ho = hornblende, En = enstatite, An = anorthite, Ch = chlorite, Ma = magnetite.

V.2.2 Major and trace element geochemistry

Twelve samples of unweathered amphibolite, amphibole-bearing pyroxenite and amphibole-bearing gabbro were analyzed for whole-rock major and trace element geochemistry (Table 1). Mg and Fe whole-rock concentrations co-increase from 5-10 wt% MgO and 4-8 wt% FeO in amphibolitic gabbro to 15-20 wt% MgO and 9-11 wt% FeO in amphibolite, and up to 25 wt% MgO and 15 wt% FeO in amphibolitic pyroxenite (Figure 9A). Conversely, Mg and Al whole-rock concentrations are anti-correlated as Al_2O_3 concentrations decrease from >15wt% in gabbro to 6-11 wt% in amphibolite and down to ~3 wt% in pyroxenite. These whole-rock correlation trends for major elements are well explained by varying proportions of the principal constitutive phases, as (i) Al-rich and Mg-Fe-free plagioclase is predominant in gabbro, (ii) Al-Fe-Mg-bearing hornblende is predominant in amphibolite and (iii) Al-poor and Mg-Fe-rich enstatite is predominant in pyroxenite. Similar to Al, Ca and Na whole-rock concentrations decrease from amphibolite to pyroxenite owing to increasing proportion of Ca-Na-poor enstatite at the expense of Ca-Na-bearing hornblende. In gabbro, Ca and Na whole-rock content may vary significantly depending both on the relative proportion of plagioclase and hornblende, and on the Ca/Na ratio of plagioclase. Ti concentration is maximum in amphibolite reaching up to 1.3 wt% TiO_2. Mineral chemistry analysis suggests that hornblende is the predominant carrier of Ti in amphibolite, although significant contribution of accessory titanite and/or Fe-Ti oxides to the whole-rock Ti budget is not excluded.

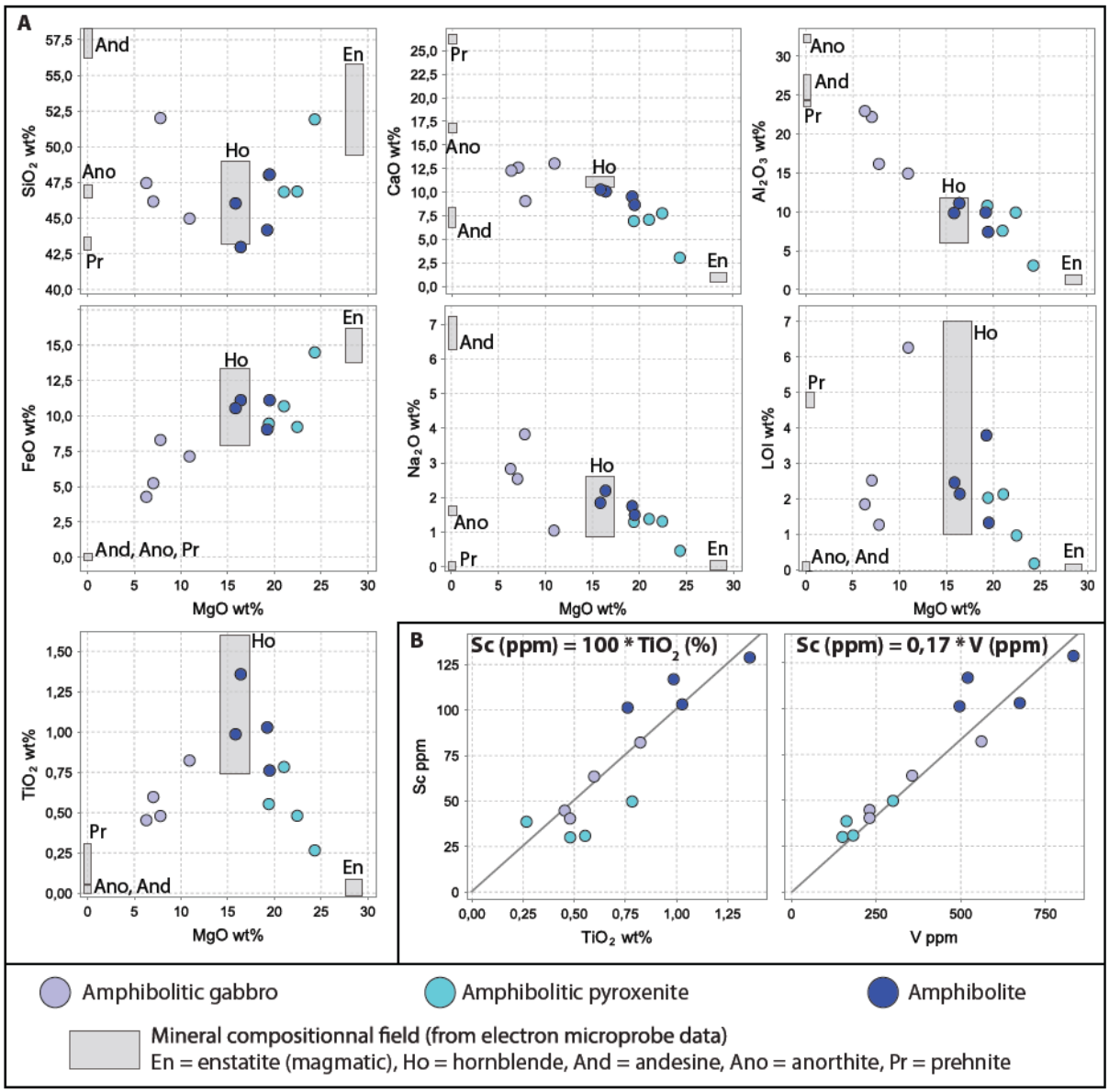

Figure 9: Whole-rock geochemistry data for mafic-ultramafic intrusive rocks (amphibolitic gabbro, amphibolitic pyroxenite, amphibolite). (A) Plots of SiO_2, CaO, Al_2O_3, FeO, Na_2O, LOI and TiO_2 (wt%) against MgO (wt%). Grey rectangles indicate mineral compositions from electron microprobe data. (B) Plots and correlations of Sc (ppm) against TiO_2 (wt%) and V (ppm).

Similar to major elements, Sc exhibits large variations of concentration in mafic-ultramafic intrusive rocks, from 30-50 ppm in pyroxenite to 40-80 ppm in gabbro and 100-130 ppm in amphibolite (Figure 9B). LA-ICP-MS analysis (Figure 10) indicates that Sc is dominantly hosted by hornblende with Sc concentrations ranging from 50 to 180 ppm and to a lesser extent by enstatite (20-25 ppm), while other mineral phases (plagioclase, Fe-Ti oxides) yield low Sc concentrations

(< 5 ppm). The whole-rock Sc content of unweathered intrusive rocks therefore depends both on the relative proportion and the Sc content of hornblende. Noteworthily, amphibolite (>90 vol% hornblende) typically contain Sc-rich hornblende (>100 ppm), so that the whole-rock Sc content of amphibolite is accordingly high. Sc-rich hornblende also occurs in some gabbro and microgabbro occurrences as those identified in Nakéty and Tiébaghi, although the large proportion of Sc-poor plagioclase in gabbros dilute and buffer the contribution of Sc-rich hornblende to the whole-rock Sc content. In contrast, hornblende-bearing pyroxenite, together with some other gabbro occurrences identified in N'Go, contain hornblende with lower Sc content (50-80 ppm), so that the whole-rock Sc content of pyroxenite does not exceed 50 ppm despite significant proportion of hornblende in the mineral assemblage.

Importantly, whole-rock Sc concentrations are well correlated with Ti and V concentrations (Figure 9B), so that the Sc content of mafic-ultramafic intrusive rocks may be approximatively estimated from the Ti and V concentrations as following:

(3) $Sc\ (ppm) = 100 * TiO_2\ (wt\%) = 0.17 * V\ (ppm)$

As revealed by mineral chemistry analysis (Figure 10), these whole-rock correlation trends are best explained by the co-variation of the Sc, V and Ti content of hornblende, which is the predominant mineral host for these elements. At the mineral scale, the Sc content of hornblende may be estimated from the Ti, V but also the Fe content of hornblende, as following:

(4) $Sc\ (ppm) = 0.017 * Ti\ (ppm) = 0.16 * V\ (ppm) = 163 * Fe\ (wt\%)$

Whereas Sc, Ti and V and predominantly hosted by hornblende so that their co-variations in hornblende directly translate into whole-rock correlation trends, Fe is hosted both by hornblende and enstatite, and the whole-rock Fe content cannot be indicative of the Sc content except for monomineralic amphibolite.

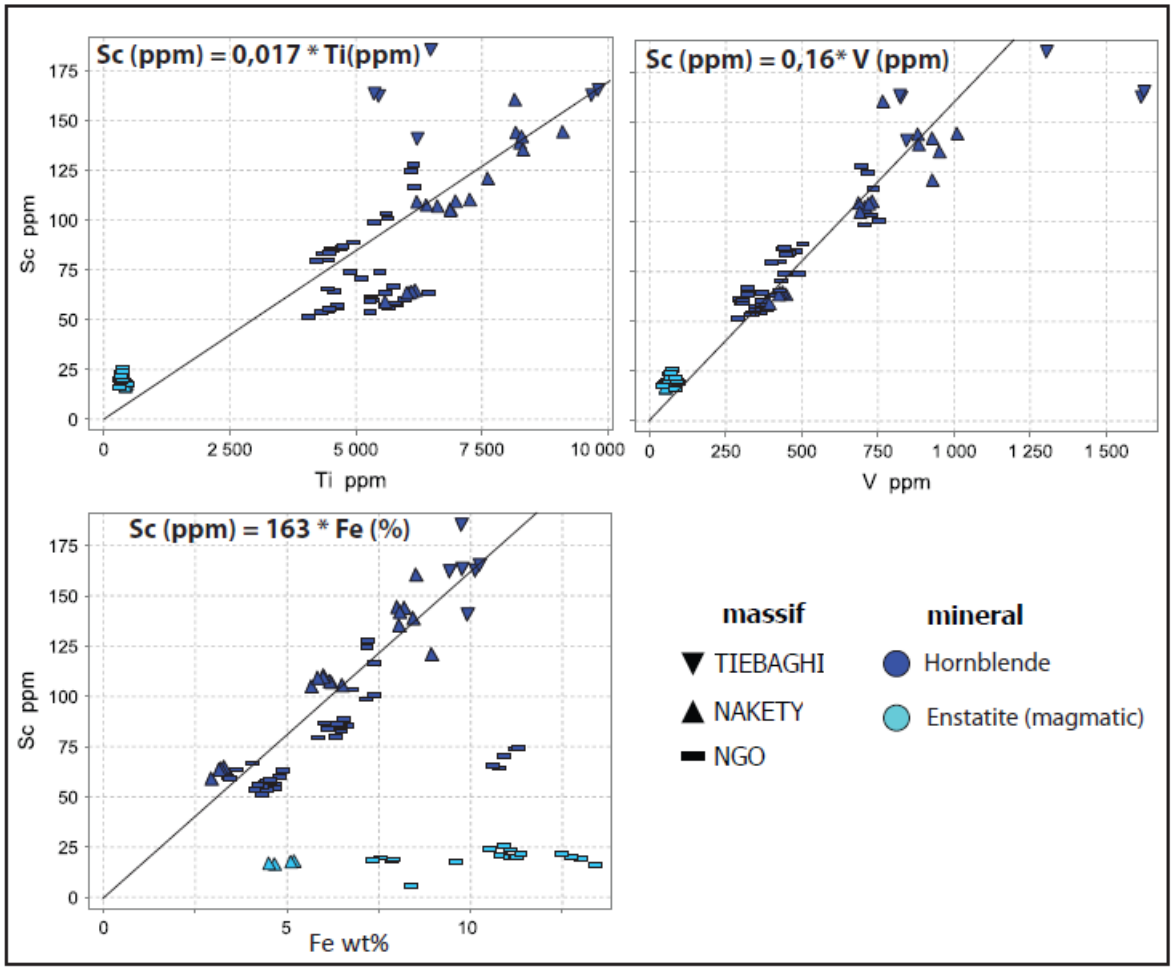

Figure 10: Plots and correlations of Sc (ppm) against Ti, V (ppm) and Fe (wt%) in magmatic minerals (enstatite and hornblende) from LA-ICP-MS data.

6 Scandium in laterites

6.1 Peridotite-hosted Ni-Co laterites

6.1.1 Paragenetic sequence

Lateritisation of peridotites is characterized by the development of several alteration facies from the bedrock to the ferricrete and is associated with complex mineral and textural transformations (Figure 11). The paragenetic sequence commonly observed in peridotite-derived laterite typically includes multiple stages of dissolution of primary silicates and formation of secondary silicates and oxides (Figure 12). At the bedrock – rocky saprolite interface, dissolution of mantellic silicates (olivine, pyroxene) is associated with the development of secondary goethite (referred to as

skeletal goethite, Go-sk) along silicate grain boundaries and crystallographic planes (Figure 11A-11C). Lizardite (Lz) is preserved from dissolution in the rocky saprolite although it is largely transformed into secondary, nickeliferous serpentine/talc-like (Lz-ni) either along fractures (Figure 11A) or through pervasive replacement (Figure 11B, 11C). Locally, accessory quartz and/or smectites may form as infills of pre-existing silicates (Figure 11C) but these are in turn rapidly dissolved upwards in the sequence. Some atypical clay-rich laterite such as those developed at Tiébaghi exhibit well-developed smectitic zones mostly consisting of Ni-bearing nontronite pseudomorphing pre-existing silicates (Figure 11D). However, in most investigated profiles elsewhere in New Caledonia, the rocky saprolite directly grades upwards into the earthy saprolite wherein most (>80 vol%) of the primary and secondary serpentines are epigenised into goethite (Go-lz) (Figure 11E). Fine-grained goethitic material derived from the overlying laterite (Go-lt) may occur as mechanic infill of voids and notably within dissolved/skeletized silicates (Figure 11F). The transition between the earthy saprolite and the laterite is marked by the accumulation (up to ~5 vol%) of Mn-Co-Ni oxides mostly represented by lithiophorite (Lp) which develops at the expense of epigenetic goethite Go-lz (Figure 11G). Upwards, the yellow laterite is characterized by the progressive compaction and destruction of pre-existing structures through the fragmentation of skeletal (Go-sk) and epigenetic (Go-lz) goethite (Figure 11H). These fragments are loosely cemented by fine grained, lateritic goethite (Go-lt) that likely underwent several stages of fragmentation, dissolution and reprecipitation (Figure 11I). The transition from the yellow to the red laterite is associated with the formation of fine grained lateritic hematite (He-lt) at the expense of the lateritic goethite matrix (Go-lt), together with the progressive decrease in size and abundance of the remaining skeletal / epigenetic goethite and Mn-Co-Ni oxide clasts (Figure 11J). Eventually, the red laterite is capped by the ferruginous hardcap or ferricrete. The basal portion of the ferricrete is usually autochtonous and is characterised by the crystallization of euhedral goethite (Go-fe, up to ~5µm) and hematite (He-fe, up to 1µm) at the expense of pre-existing oxides (Figure 11K). The upper portion of the ferricrete usually consists of accumulated goethitic and hematitic pisoliths (Go-pi and He-pi) cemented by a goethite-rich

matrix (Figure 11L). Overgrowth of pisolithic goethite on hematite cortex is commonly observed. Also, large (3mm-1cm) goethite pisoliths may exhibit marked zonation textures indicating successive growth stages. Throughout the lateritic profile, accessory magnetite and chromiferous spinel are mostly resistant to weathering and residually accumulate upwards.

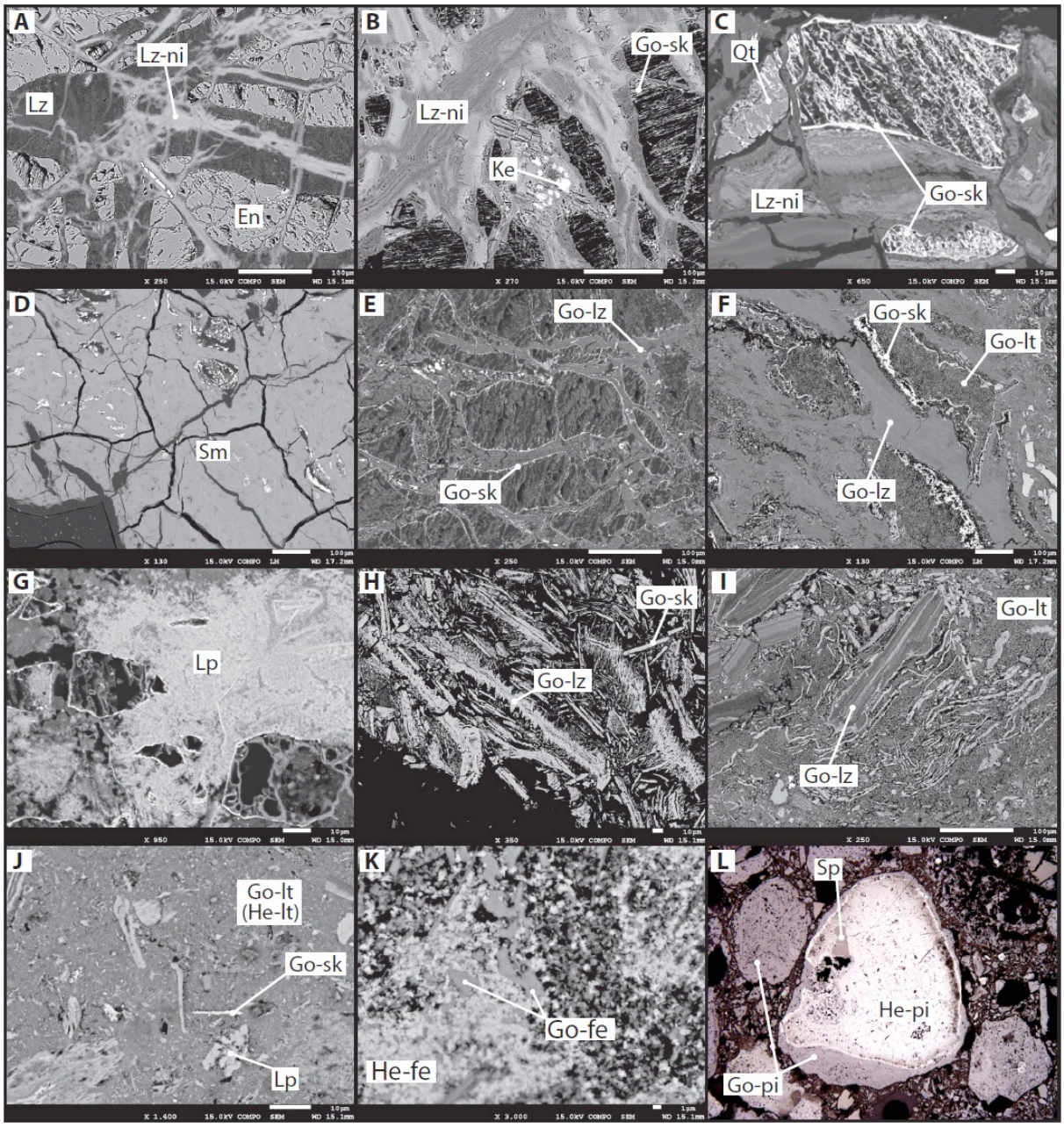

Figure 11: Backscattered Electron (BSE) microphotographs: (A) Bedrock – rocky saprolite interface: onset of olivine/pyroxene dissolution and formation of secondary Ni-bearing serpentine/talc-like (Lz-ni) at the expense of lizardite (Lz). (B-C) Rocky saprolite: effective dissolution of olivine/pyroxene, formation of skeletal goethite (Go-sk) preserving the structure of

primary silicates, together with secondary Ni-bearing serpentine/talc-like (Lz-ni) and kerolite (Ke). (D) Atypical clay-rich zone from Tiébaghi laterites: replacement of primary and secondary serpentines by smectites (Sm), mostly Ni-bearing nontronite. (E-F) Earthy saprolite: epigenisation of serpentines into goethite (Go-lz) and onset of void infill by fine-grained lateritic goethite (Go-lt). (G) Transition laterite: accumulation of Mn-Co-Ni oxides, mostly lithiophorite. (H-I) Yellow laterite: fragmentation of pre-existing structures. (J) Red laterite: Advanced texture obliteration, decrease in size and abundance of the remaining skeletal / epigenetic goethite and Mn-oxide clasts, and formation of lateritic hematite (He-lt) within the lateritic goethite (Go-lt) matrix. (K) Basal allochtonous ferricrete: formation of crystallised ferricritic goethite (Go-fe) and hematite (He-fe). (L) Pisolithic horizon: formation of pisolithic goethite (Go-pi) locally overgrowing pisolithic hematite (He-pi) and/or encapsulating Cr-spinel (Sp) relics.

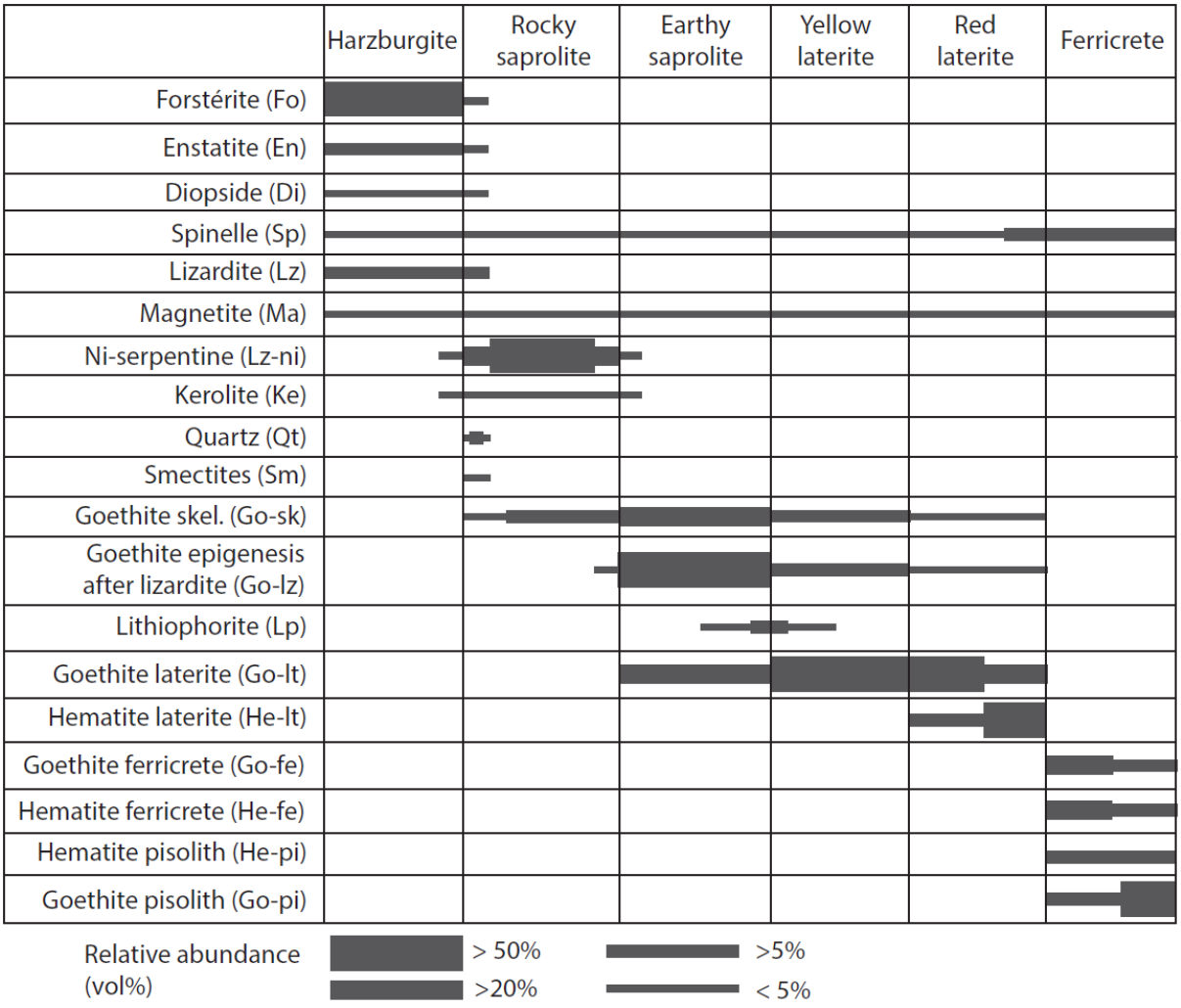

Figure 12: Evolution of mineral relative abundances and assemblages along a typical lateritic sequence developed after harzburgite.

6.1.2 Distribution of major and trace elements

The present section first describes the whole-rock geochemical changes along three profiles selected for their representativeness: (i) the dunite-derived PZ1B profile (17 samples) from Cap Bocage (Figure 13), (ii) the harzburgite-derived OPB7 profile (16 samples) from Koniambo (Figure14) and (iii) the lherzolite-derived TIEA profile (14 samples) from Tiébaghi (Figure 15). Elementary correlations obtained from whole-rock analysis (Figure 16) are then presented for the entire dataset that includes 105 samples collected along ten peridotite-derived lateritic profiles (Table 1). In situ minor (Si, Al, Cr, Ni; EPMA WDS analysis) and trace (Sc; LA-ICP-MS analysis) element concentrations in goethite and hematite along the OPB7 profile are finally documented (Figure 17) and discussed with regards to whole-rock geochemical data.

Typical oxide-rich lateritic profiles PZ1B and OPB7 exhibit characteristic geochemical distribution patterns. In both profiles, the rocky to earthy saprolite interface constitutes the most prominent geochemical transition with the sharp depletion of SiO_2 and MgO from 40 to <5-10 wt%, and the concomitant increase in Fe_2O_3 from ~7 to ~60 wt% (Figure 13, 14). Contrasting with oxide-rich laterites, lateritic profiles from Tiébaghi exhibit clay-rich saprolitic zones characterized by more progressive Mg depletion and Fe enrichment (Figure 15). From the base of the earthy saprolite up to the ferricrete, Fe_2O_3 concentrations further increase up to ~70wt% together with further decrease of the SiO_2 and MgO contents. Similar to Fe, a number of elements including Al, Cr, Mn, Ni, Co, Sc, V and REEs exhibit a ~tenfold enrichment in the lateritic profile compared to the parent peridotite. However most of these elements display different distribution patterns compared to Fe in that their maximum concentrations occur at intermediate positions within the lateritic profile. Ni usually reaches maximum concentrations in the rocky saprolite (~2 wt%) and almost linearly decreases in concentration upwards in the profile. Similarly, Mn and Co concentrations are maximum in the transition laterite and decrease upwards, while Al and Sc concentrations are

maximum in the yellow laterite (Figure 13, 14). The initial Sc content of the parent peridotite strongly controls the maximum Sc grade of its lateritised derivatives, so that the dunite-derived laterite from the PZ1B profile yields a maximum Sc grade of ~60 ppm, while the harzburgite- and lherzolite-derived laterites from the OPB7 and TIEA profiles, respectively, yield maximum Sc grades of ~100 ppm.

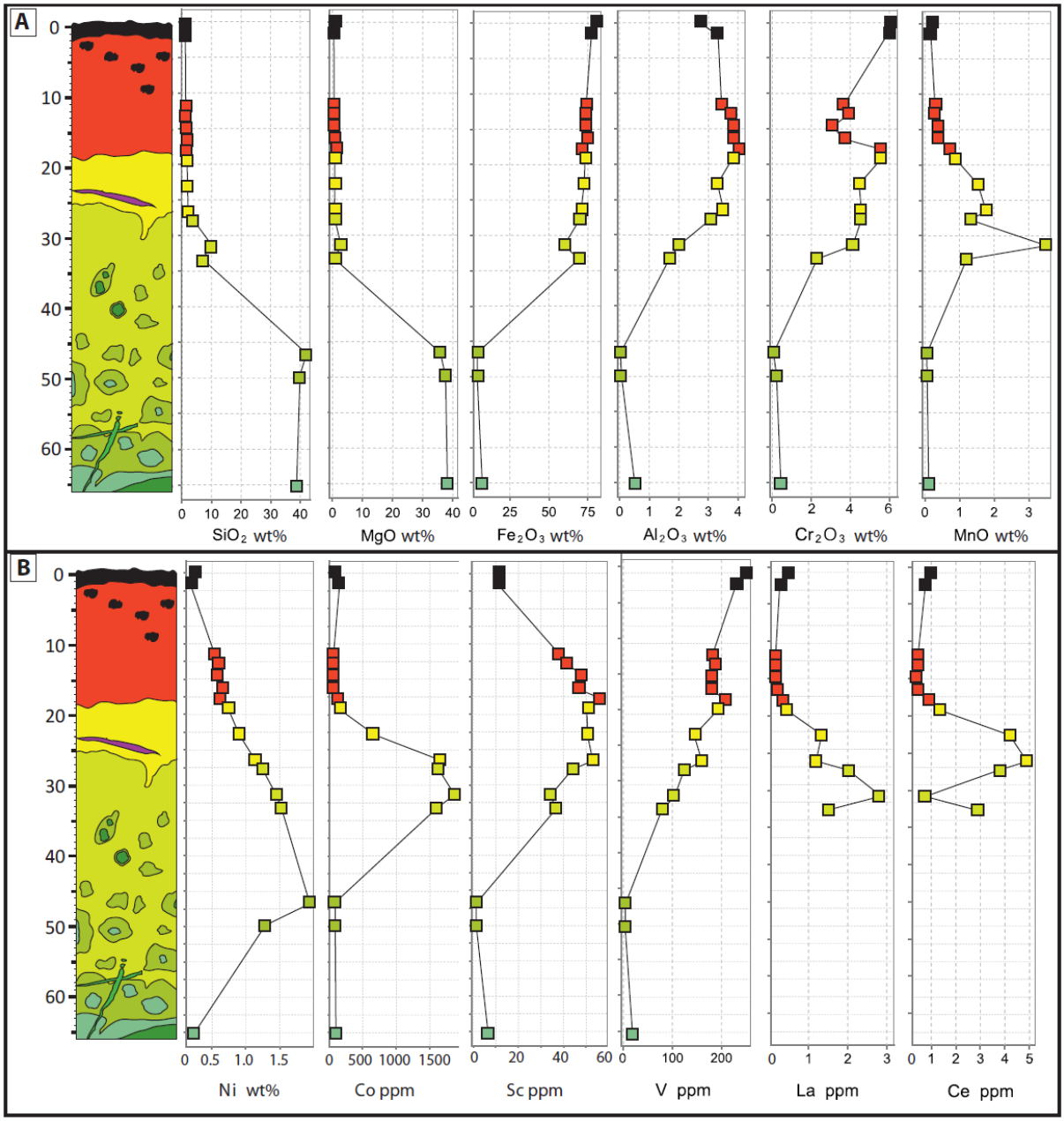

Figure 13: Geochemical evolution along dunite-derived lateritic profile PZ1B (Cap Bocage): (A) Major oxides: SiO_2, MgO, Fe_2O_3, Al_2O_3, Cr_2O_3, MnO (wt%), (B) Economic elements: Ni (wt%), Co (ppm), Sc (ppm), trace and LREE: V, La, Ce (ppm).

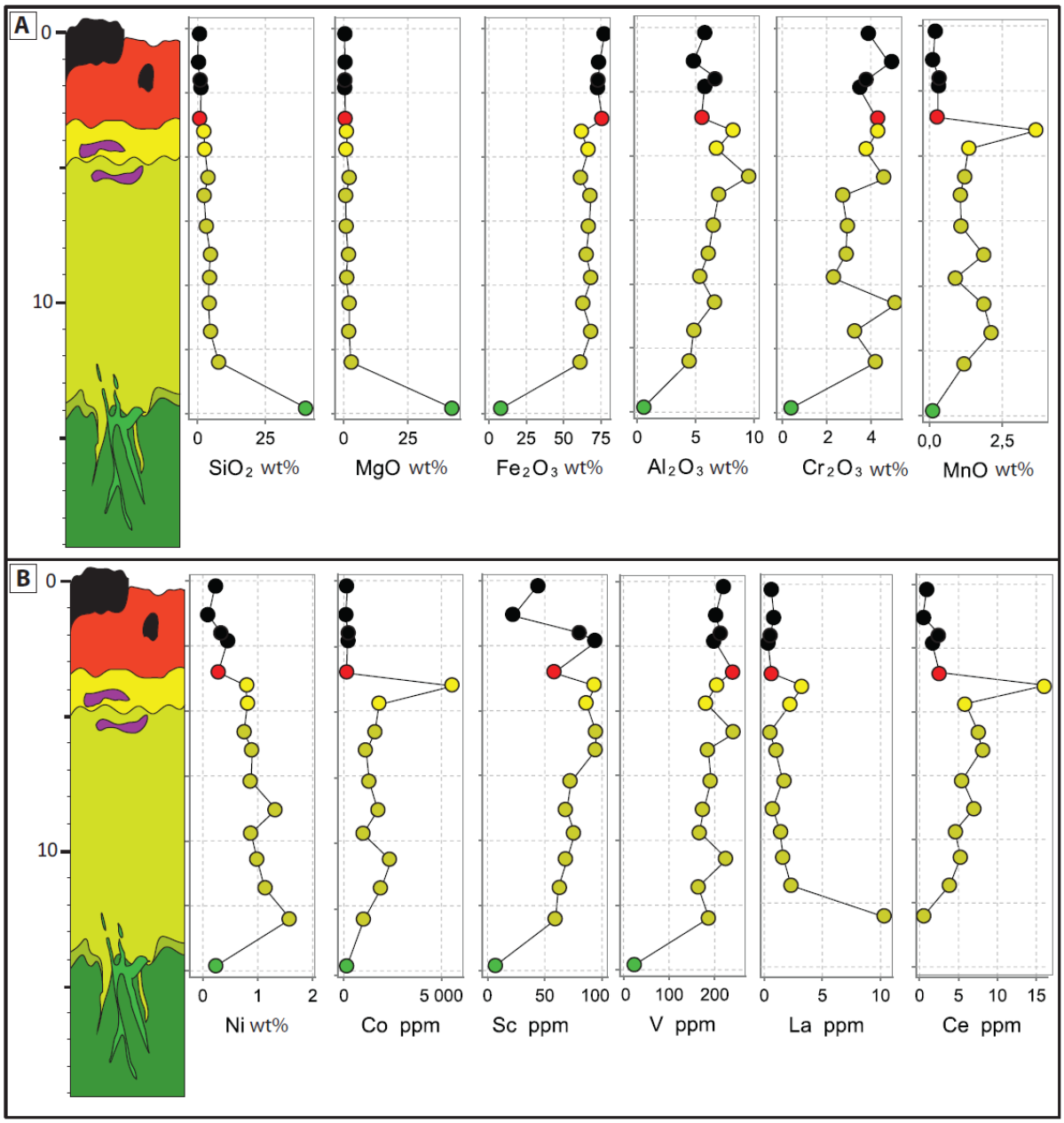

Figure 14: Geochemical evolution along harzburgite-derived lateritic profile OPB7 (Koniambo): (A) Major oxides: SiO_2, MgO, Fe_2O_3, Al_2O_3, Cr_2O_3, MnO (wt%), (B) Economic elements: Ni (wt%), Co (ppm), Sc (ppm), trace and LREE: V, La, Ce (ppm).

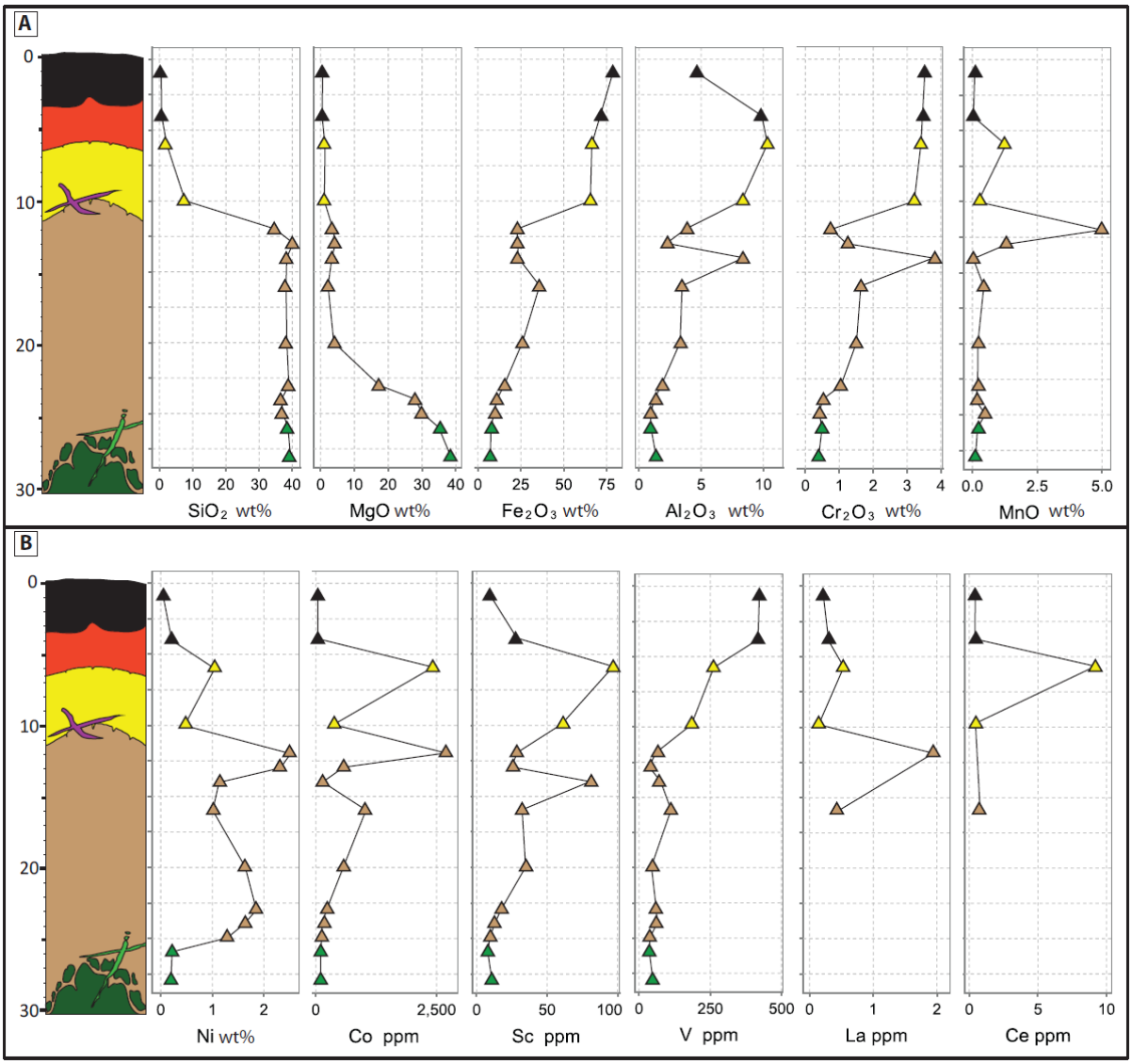

Figure 15: Geochemical evolution along lherzolite-derived lateritic profile TIEA (Tiébaghi): (A) Major oxides: SiO_2, MgO, Fe_2O_3, Al_2O_3, Cr_2O_3, MnO (wt%), (B) Economic elements: Ni (wt%), Co (ppm), Sc (ppm), trace and LREE: V, La, Ce (ppm).

Plot of Sc against Fe_2O_3 concentrations for the nine investigated lateritic profiles (Figure 16A) indicates that Sc and Fe are positively correlated from the parent rock up to the lower portion of the earthy saprolite ($Fe_2O_3 \leq 60$ wt%). There, the Sc content may be approximatively estimated from the Fe_2O_3 concentrations as following:

(5) Sc (ppm) = 1.0* Fe_2O_3 (wt%)

Above in the profiles (Fe_2O_3 > 60 wt%), Sc concentrations are largely variable and discorrelated with Fe concentrations. From the upper portion of the earthy saprolite up to the yellow laterite, Sc is enriched compared to Fe, so that Sc grades reach 90-100 ppm in harzburgite- and lherzolite-derived peridotites while the Fe_2O_3 content does not exceed 70 wt%. In the uppermost horizons (red laterite and ferricrete), Sc is at first order anti-correlated to Fe, as Sc concentrations decrease down to ~10 ppm while Fe_2O_3 concentrations continuously increase up to 80 wt%. In contrast, Sc concentrations are positively correlated with Al and to a lesser extent with V concentrations from the parent bedrock up the red laterite, so that the Sc content may be approximatively estimated from the Al_2O_3 and V concentrations as following:

(6) Sc (ppm) = 11.7* Al_2O_3 (wt%) = 0.32*V (ppm)

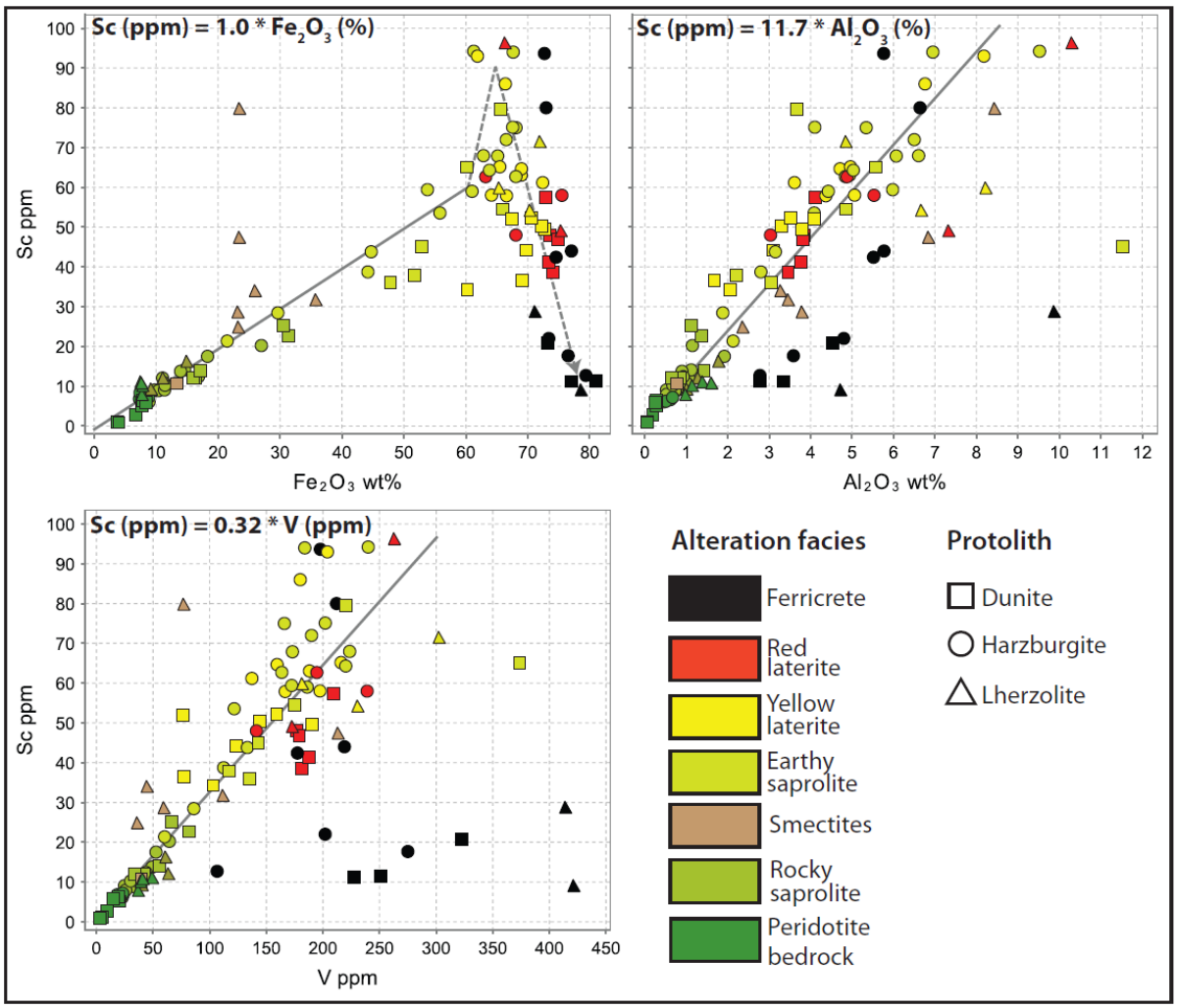

Figure 16: Plots of Sc (ppm) as a function of Fe_2O_3, Al_2O_3 (wt%) and V (ppm) along the 9 investigated peridotite-derived lateritic profiles (whole-rock data).

At the mineral scale, in situ analyses of iron oxides and oxyhydroxides from the OPB7 profile reveal that the different generations of goethite and hematite (defined from optic and scanning electron microscopy, see section VI.1.1) yield specific minor and trace element concentrations. Early-formed skeletal goethite yields the highest Si and Ni concentrations (~2 and 1 wt%, respectively) together with low Al and Cr concentrations (~1 and 0.3 wt%, respectively) (Figure 17A). Subsequent formation of epigenetic and lateritic goethite is associated with a decrease of the Si and Ni concentrations and an increase of the Al and Cr concentrations. Late-stage ferricritic and pisolithic goethite and hematite are characterized by further depletion of Si and Ni, together with a major increase of the Cr content (up to 5 wt%) and variable Al concentrations. Also, as revealed by LA-ICP-MS analysis, in situ Sc concentrations of goethite and hematite strongly depends on their vertical position along the lateritic profile (Figure 17B). Variations of Sc concentrations in goethite, and to a lesser extent hematite, largely explain the distribution of whole-rock Sc concentrations, so that the distribution of Sc in the laterite profile is mostly controlled by variations of the Sc content in goethite, rather than by the relative proportion of goethite and hematite.

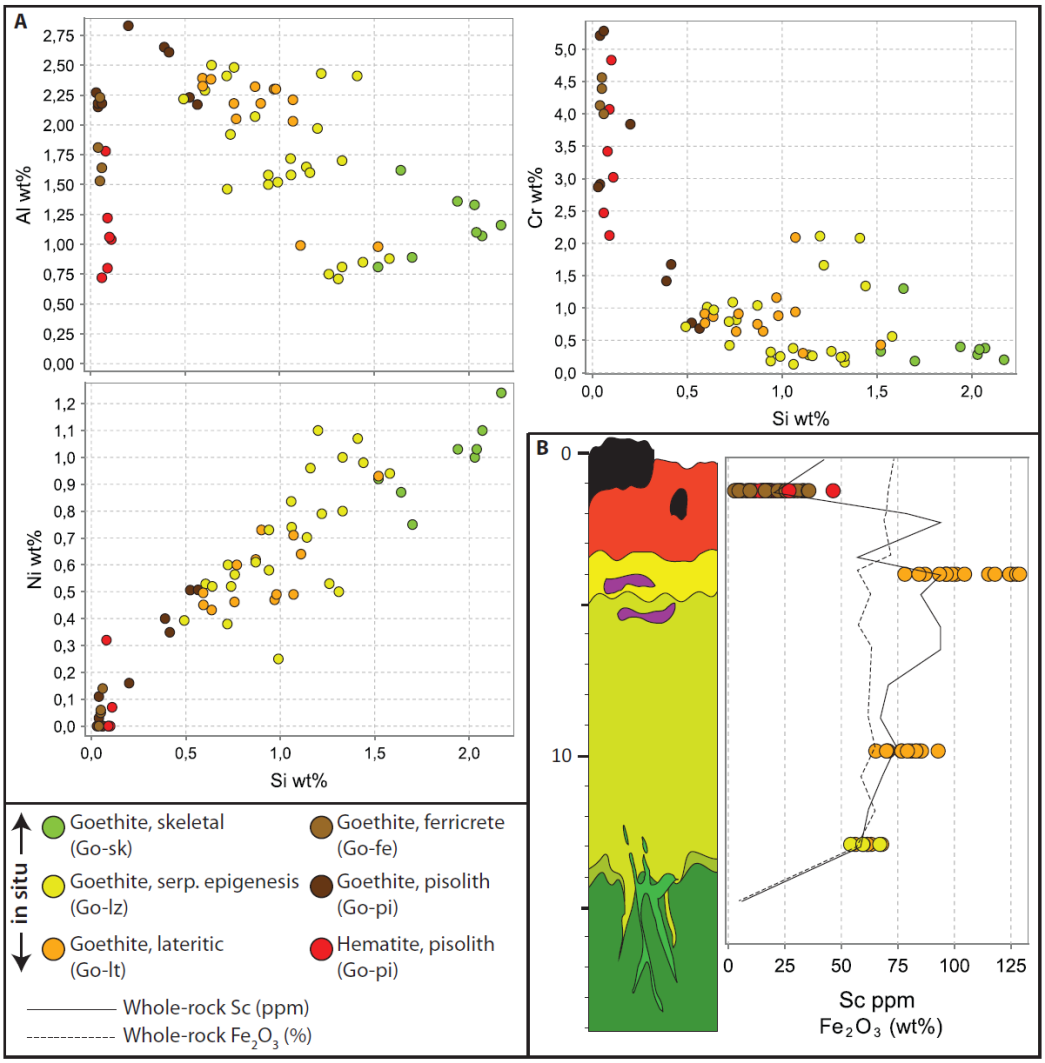

Figure 17: (A) Plots of Al, Cr and Ni as a function of Si (wt%) in goethite and hematite from the harzburgite-derived OPB7 profile, Koniambo (WDS data). (B) Evolution of the Sc content of goethite in the OPB7 profile (LA-ICP-MS data) and comparison with whole-rock Sc and Fe_2O_3 concentration patterns.

6.2 Mafic-ultramafic intrusive rocks

6.2.1 Paragenetic sequence

Weathering of mafic and ultramafic intrusive rocks (amphibolites, pyroxenites and gabbros) results in the dissolution of primary magmatic minerals and the formation of specific secondary mineral assemblages. In amphibolites and amphibole-bearing pyroxenites, dissolution of

hornblende commonly initiates along crystallographic planes and is associated with the formation of early-stage skeletal goethite. Skeletal goethite networks are in turn coated either by euhedral gibbsite (Figure 18A) or by poorly crystallized kaolinite (Figure 18B), each individual goethitic compartment exhibiting either gibbsite or kaolinite coatings, but not both. Locally, both gibbsite and kaolinite may however occur within a single compartment. In such a case, textural relationships commonly argue for a latter formation of gibbsite relative to kaolinite (Figure 18E), although rare occurrences of kaolinite developed after gibbsite may also be observed (Figure 18F). Early-stage alteration of enstatite may result in the formation of smectites (Figure 18C), which are in turn readily transformed into kaolinite (Figure 18G). Further development of alteration leads to increased development of goethite at the expense of kaolinite (Figure 18E-18H), eventually resulting in the formation of a matured, goethite + gibbsite assemblage (Figure 18I). Contrasting with amphibolites and pyroxenites, weathering of gabbros commonly result in the formation of kaolinite rather than Al-oxides (Figure 18J), and, more importantly, the formation of hematite instead of goethite (Figure 18K, 18L). There, hematite typically postdates kaolinite, as indicated by overgrowth (Figure 18K) and replacement (Figure 18L) textures. Such replacement of kaolinite by hematite argue for the downward remobilization of iron, as previously characterized in some african lateritic profiles (Ambrosi et al., 1986).

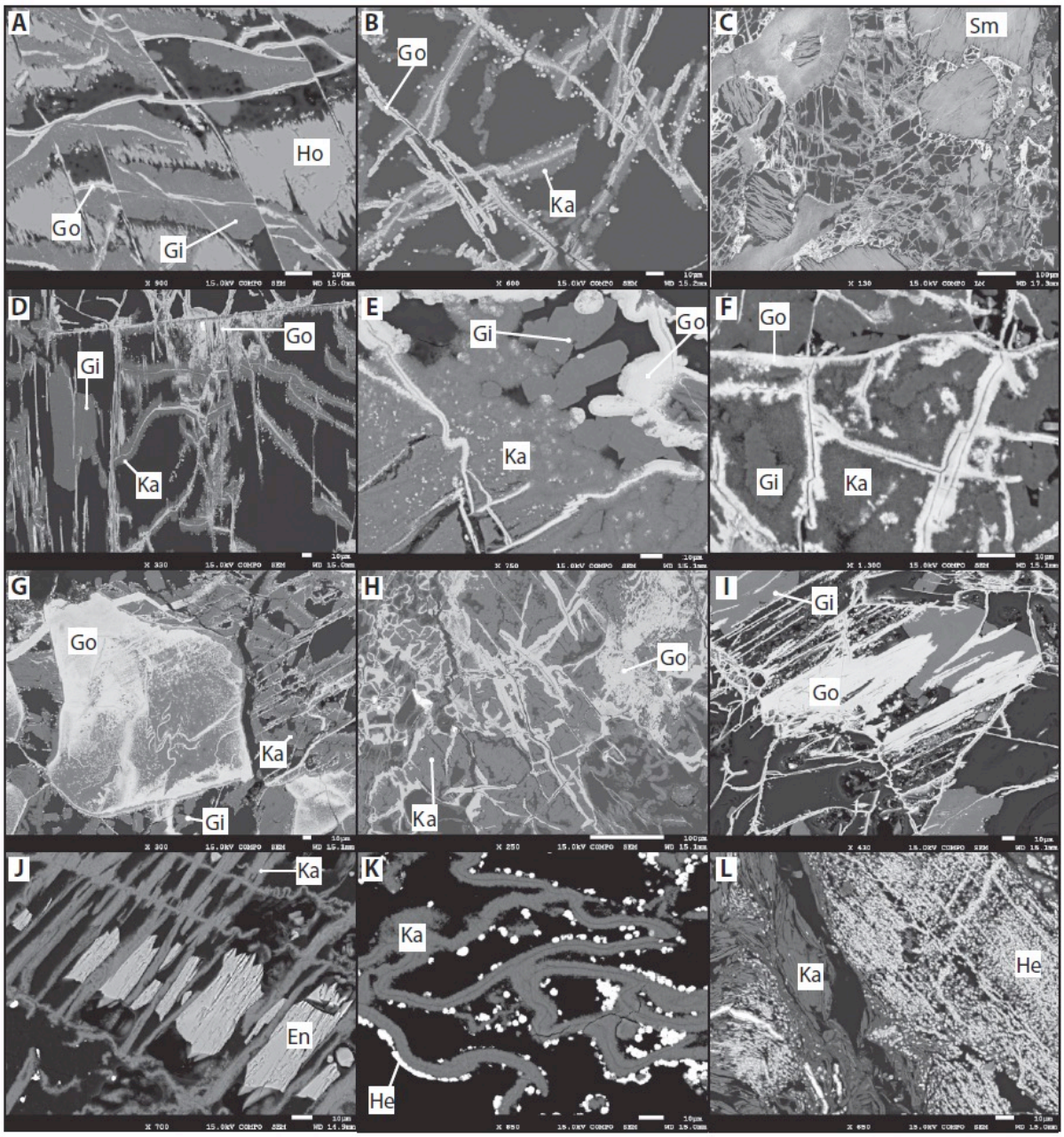

Figure 18: Backscattered Electron (BSE) microphotographs: (A-I) amphibolite-derived saprolite. (J-L) gabbro-derived saprolite and laterite. Ho = hornblende, Go = goethite, Gi = gibbsite, Ka = kaolinite, En = enstatite, He = hematite.

6.2.2 Distribution of major and trace elements

The saprolitisation of amphibolite (and amphibole-bearing pyroxenite) dykes is associated with major depletion of mobile cations Si, Mg and Ca, together with the residual enrichment of Fe, Al

and Cr (Figure 19A). Owing to the formation and relative preservation of kaolinite in saprolitized amphibolites, the observed depletion in Si is progressive and delayed compared to the sharp depletion in Mg (and Ca), contrasting with typical peridotite-derived laterites wherein both Si and Mg exhibit sharp and congruent depletion. Fe and Cr enrichments are maximal at the top of the alteration profile, whereas Al concentrations are maximal at an intermediate position within the profile. Such distribution patterns are similar to those observed in typical peridotite-derived laterites. Economic elements Ni, Co and Sc also exhibit similar distribution patterns compared to those observed in Ni-laterites: Ni concentrations are maximum in the lower saprolite although not exceeding 1 wt%. Co and Sc maximum concentrations occur at intermediate position within the profile (Figure 19B). Importantly, saprolitized amphibolites exhibit a two- to threefold increase in Sc concentrations compared to the parent rock, so that fertile amphibolites (≥ 100 ppm Sc) alter to saprolite with Sc concentrations up to ~300 ppm. As observed in Ni-laterites, Sc in saprolitized amphibolites exhibit distribution patterns similar to those of Al and V.

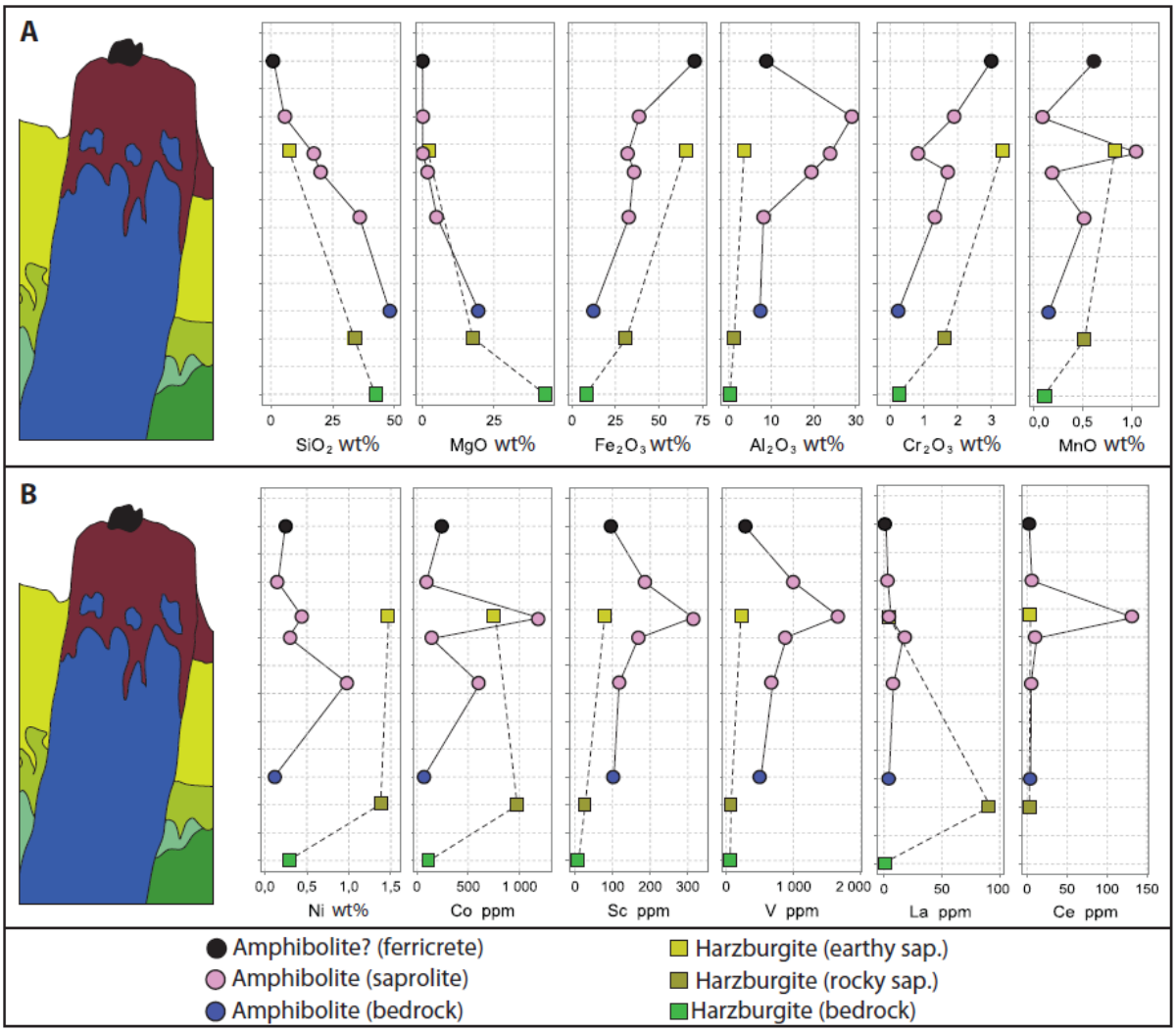

Figure 19: Geochemical evolution along amphibolite-derived laterite profile NGPB (N'Go): (A) Major oxides: SiO_2, MgO, Fe_2O_3, Al_2O_3, Cr_2O_3, MnO (wt%), (B) Economic elements: Ni (wt%), Co (ppm), Sc (ppm), trace and LREE: V, La, Ce (ppm).

At the mineral scale, WDS elementary mapping of mineral assemblages in saprolitized amphibolites indicate that Sc is essentially hosted by early-stage skeletal goethite and late-stage goethite formed after kaolinite, and to a much lesser extent by kaolinite (Figure 20). In saprolites developed after fertile (> 100 ppm Sc) amphibolites, goethite yields Sc concentrations up to about 0.08 wt% (i.e. 800 ppm) together with Ni and Co concentrations up to 1 and 0.03 wt%, respectively. There, the spatial distribution of V appears similar to that of Sc. In contrast, Ti is

mostly hosted by early-formed skeletal goethite and is largely absent in late-stage patchy goethite formed after kaolinite.

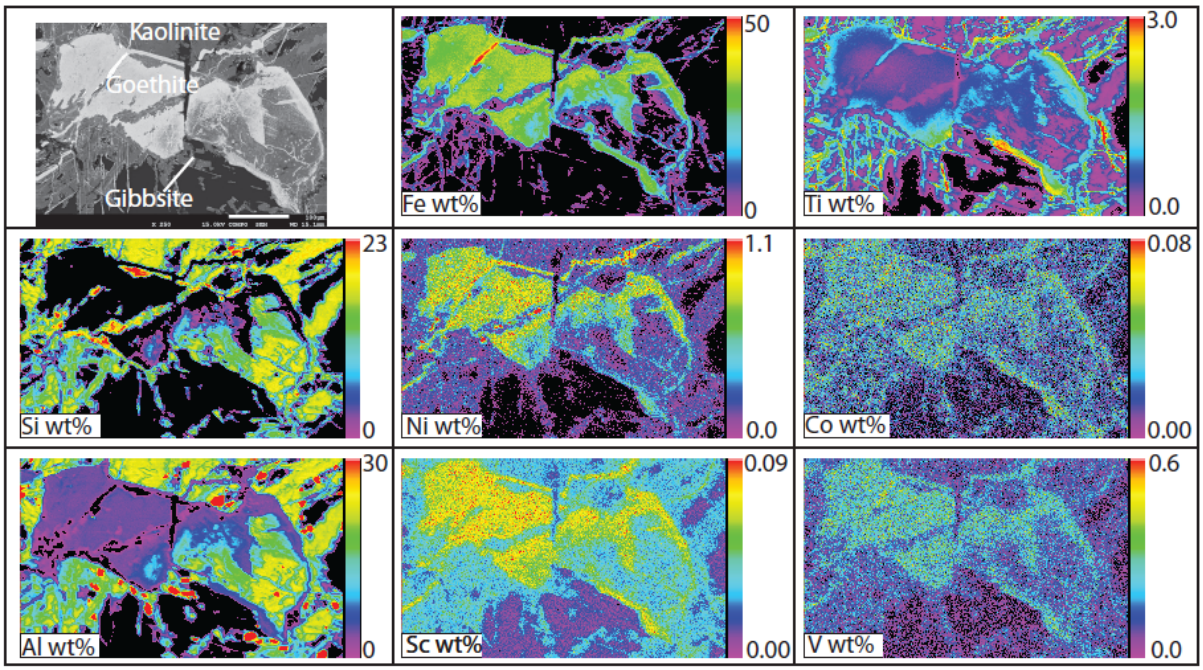

Figure 20: Quantitative elementary maps (Fe, Ti, Si, Ni, Co, Al, Sc, V; wt%) of a goethite – kaolinite – gibbsite mineral assemblage developed in amphibolite-derived saprolite (NGPB profile, N'Go).

Contrasting with goethite-bearing saprolitized amphibolites, hematite-bearing laterites developed after gabbros exhibit relatively low (usually < 50 ppm) whole-rock Sc concentrations (Figure 21), i.e. lower than their unweathered counterparts (40-80 ppm, see Figure 9 section V.2.2), suggesting that Sc is expulsed during the weathering of gabbros. Such remobilization of Sc from gabbros is supported by the anomalously elevated Sc concentrations identified in footwall peridotite-derived laterites wherein the Sc content exceeds 150-200 ppm (Figure 21). There, the observed Sc over-enrichment extends down to ~2 meters below the base of the gabbro intrusive bodies.

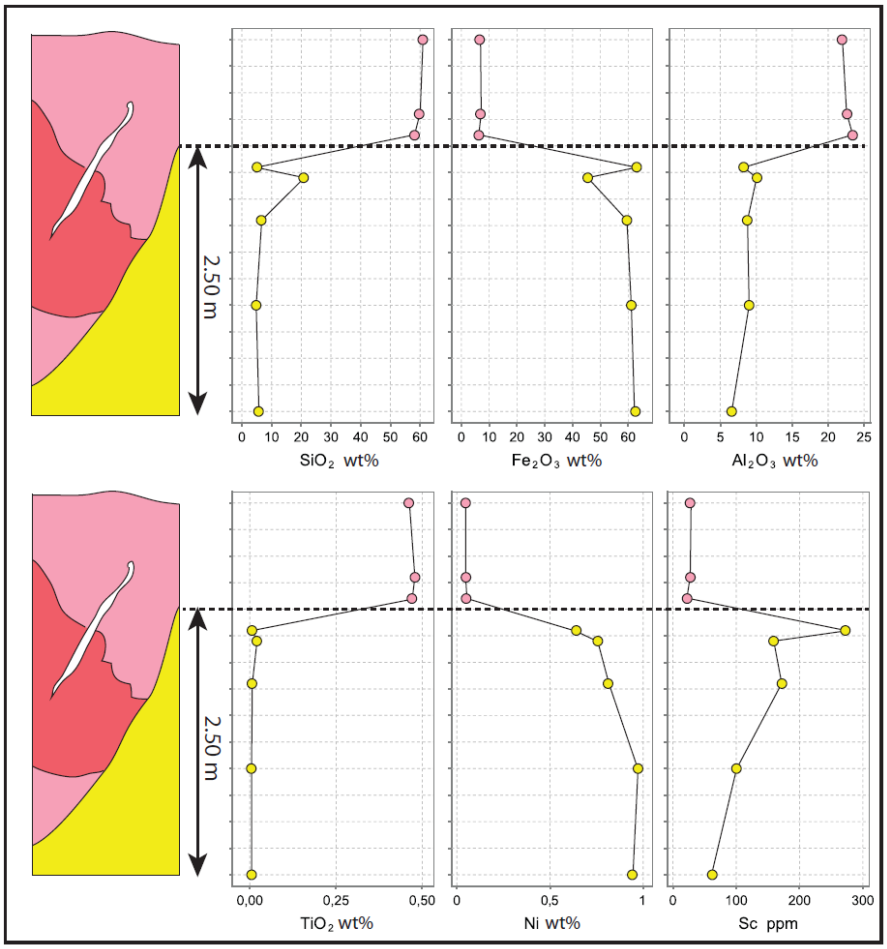

Figure 21: Geochemical evolution along gabbro-derived laterite profile KNGA (Koniambo): Major oxides: SiO_2, Fe_2O_3, Al_2O_3, TiO_2 (wt%), economic elements: Ni (wt%), Sc (ppm).

7. Discussion and implications for Sc exploration

This study aims to document the distribution of Sc in New Caledonian laterites and to assess the main factors controlling its distribution in lateritic profiles encompassing for the diversity of protoliths and alteration styles. Critical conditions for the development of Sc-rich zones with potential economic interest are discussed in the following section based on field and analytical investigations.

7.1 Synthesis of field and analytical observations

Combination of field observation, mineral characterization, bulk rock and mineral geochemical data reveals a remarkable evolution of the Sc mineral hosts and abundances in lateritic profiles of New Caledonia. Unweathered mafic and ultramafic rocks exhibit a large range of Sc concentrations

from <5 ppm in dunite to >10 ppm in lherzolite and up to 100 ppm or higher in amphibolite, resulting from variable contributions of Sc-bearing primary phases (mostly enstatite in peridotites and hornblende in intrusive rocks). The lateritisation of peridotites results in the progressive increase of Sc concentrations upwards in the profile so that maximum Sc concentrations are reached in the goethite-dominated yellow laterite, representing a ~tenfold enrichment compared to the parent peridotite. Whereas Sc concentrations co-increase with Fe concentrations from the bedrock to the earthy saprolite, Sc commonly exhibits a relative enrichment compared to Fe in the yellow laterite and a relative depletion in the red laterite and ferricrete. Such distribution appears more similar to that of Al or V. In these oxide-rich horizons, whole-rock Sc concentrations are mostly controlled by the Sc content of goethite which significantly varies from the earthy saprolite to the ferricrete. The Sc content within these horizons is not only controlled by the relative proportion of goethite and hematite, as proposed by Chassé et al. (2017), but also and to a much larger extent by the Sc content of goethite itself.

In saprolitized amphibolites, Sc is also essentially hosted by goethite. There, owing to the higher Al content of the parent rock compared to peridotites, goethite does not represent the predominant secondary phase but occur in association with Sc-poor kaolinite and/or gibbsite. Consequently, the Sc concentration factor from unweathered amphibolites to their weathered derivatives is about 2 to 3 (i.e. lower than the tenfold increase observed in peridotite-derived laterites). Yet, weathering of some Sc-rich (>100 ppm) amphibolites leads to the formation of goethite–gibbsite–bearing saprolite that yields the highest Sc content recognized so far in New Caledonia (up to >300 ppm Sc), with goethite being the predominant Sc host with up to ~800 ppm Sc. In contrast, the lateritisation of gabbros leads to the formation of hematite–kaolinite–dominated assemblages and is associated with significant expulsion of Sc. Remobilised Sc is trapped in the surrounding goethite-rich laterite derived from peridotite, leading to important Sc over-enrichment up to >150-200 ppm within a few meters from the gabbro salbands.

7.2 Preliminary genetic model and critical controls for the formation of Sc-rich laterites

Field and analytical data documented in the present contribution allow to propose a preliminary genetic model for Sc enrichment in laterites developed after mafic and ultramafic rocks of New Caledonia. In peridotite-derived lateritic profiles, the dissolution of primary silicates and leaching of Si and Mg lead to the co-enrichment of Sc with other poorly mobile elements, most notably Fe, thus forming Sc-bearing secondary goethites. Such co-enrichment, recognized from the base up to the earthy saprolitic zones of the investigated lateritic profiles, is interpreted to be essentially residual with no or marginal remobilization of Sc. Upwards, the observed relative enrichment and depletion of Sc compared to Fe support a certain mobility of Sc which is, to some extent, expulsed from the uppermost horizons (red laterite and ferricrete) and accumulates downwards in the yellow laterite. Such behavior is quite similar to that of Ni in oxide-rich horizons, although the lower mobility of Sc together with its strong affinity with goethite result in its maximum accumulation at a higher position in the profile (i.e. in the yellow laterite rather than in the saprolite). With regards to Ni, the upwards decrease of Ni concentrations in oxide-rich horizons relates to its expulsion from goethite after (i) goethite ageing through successive dissolution and recrystallisation processes forming increasingly crystallised goethite and (ii) goethite dehydration to hematite in the uppermost lateritic horizons (Dublet et al., 2015; Schwertmann and Latham, 1986). Such model appears partly suitable for explaining the distribution of Sc and its maximum enrichment in the yellow laterite, providing that downward-remobilized Sc from the uppermost horizons (red laterite and ferricrete) is more readily trapped in the direclty underlying goethite-rich yellow laterite. Further support for this model arises from the observation that Sc accumulates in goethite-rich saprolitized amphibolites whereas it is largely remobilized from hematite-rich lateritized gabbros and accumulates in surrounding goethite-rich lateritized peridotites. The striking discrepancy in the nature of secondary iron carriers between peridotite- and amphibolite-derived alterites on one hand (mostly goethite) and gabbro-derived alterites (mostly hematite) on the other is facies-dependant and commonly observed down to the outcrop

scale (e.g in the South Alpha pit, Tiébaghi, Figure 4B). Such discrepancy likely results either from differences in the activity of water, pH and/or Al/Fe ratio (Tardy and Nahon, 1985; Trolard and Tardy, 1989; Ramanaidou, 1989). With regards to the activity of water, high drainage conditions in lateritic profiles favor the maintenance of unsaturated zones at great depths wherein hematite predominates over goethite. Conversely, poor drainage conditions lead to water saturation at shallower depths and favor goethite over hematite. With regards to pH, goethite formation is optimal both at low (pH=4) and high (pH=12) pH, whereas hematite formation is optimal at near neutral (pH=8) pH. Eventually, increase in the Al/Fe ratio tends to favor goethite over hematite providing that the water activity remains comprised between ~0.55 and 0.85. Among these, it is here proposed that changes in water activity represent the predominant cause for the observed mineral discrepancy at the outcrop scale. Subvertical, readily altered gabbros likely constitute preferential drain pathways for weathering fluids, allowing the maintenance of unsaturated conditions at much greater depths compared to surrounding lateritised peridotites. At the opposite, amphibolites and pyroxenites are more resistant to alteration and probably act as aquitards for both lateral and downwards fluid circulation.

It is therefore proposed that three main factors control the distribution and intensity of Sc enrichment in peridotite-, amphibolite- and gabbro-derived laterites. The first critical factor for the formation of Sc-rich zones in laterites is the occurrence of parent rocks that have a strong potential (fertility) for subsequent upgrade and mineralisation. The fertility of a given parent rock is primarily controlled by the relative proportion of Sc-bearing primary phases, mostly enstatite and hornblende in peridotites and intrusive rocks, respectively. In peridotites, significant variations in the Sc content of enstatite are also observed depending on the considered peridotitic massif, with higher concentrations observed within lherzolites of the Tiébaghi massif. In intrusive rocks, Sc-bearing hornblende exhibit very large variations of the Sc content down to the outcrop scale. The second critical element for the formation of Sc-rich laterites is the maintenance of long-lived tropical weathering allowing acidic, Si-under saturated meteoric fluids to dissolve primary minerals and leach away most cations including Si, thus favouring the concentration of iron as

goethite together with other poorly mobile elements including Sc. Third, further maturation of peridotite- and amphibolite-derived lateritic profiles favor both the dissolution/recrystallization of goethite and its dehydration into hematite, both processes likely resulting in the local remobilization and over-concentration of Sc in the directly underlying horizons. In a similar manner, the preferential hematitisation of gabbros during weathering results in the remobilization of Sc and its over-concentration in surrounding goethite-rich zones. In any case, the formation of goethite is of critical importance as it is the predominant mineral trap for Sc. The chemical speciation of Sc in goethite remains to be investigated as it probably has important implications both for further understanding of Sc mobility in laterites as well as for the fine-tuning of metallurgical Sc extraction processes. Based on XANES analysis of lateritic samples from the Syerston-Flemington Sc deposit, Chassé et al. (2017) propose that Sc is mostly adsorbed on goethite. Alternatively, from the combination of XANES and sequential chemical extractions, Munoz and Ulrich (2017) argue that Sc is mainly co-precipitated in Fe-Sc goethite solid solution.

7.3 Implications for Sc exploration and mining in New Caledonia

A possible exploration strategy for identifying peridotite-derived Ni laterites wherein the Sc content is high enough to make it a potentially attractive by-product of Ni (and Co) production includes:

- The recognition of fertile peridotitic parent rocks. Harzburgite and lherzolite are the most fertile types of peridotite as they contain significant proportions of Sc-bearing enstatite (and more marginally diopside). This study has demonstrated that Al and V are reliable pathfinder elements indicative of the Sc content in unweathered peridotites regardless their degree of serpentinisation. At the deposit scale, the analysis of the Al (and V) content of unweathered peridotites may therefore complement field-based recognition of peridotite facies, especially in strongly serpentinized zones.
- The recognition of Sc-rich lateritic horizons and their degree of overlap with Ni(-Co)-rich zones. As Sc is most enriched in the yellow laterite horizons, zones of maximum Sc enrichment do not coincide with zones of maximum Ni (and Co) enrichment. Yet,

determination of respective Ni, Co and Sc cut-off grades based on stock prices and production costs considerations may allow to identify overlapping zones wherein covalorisation of lateritic Ni, Co and Sc may be economically viable while Ni grades remain too low to be attractive for a standalone commodity production. There, as for unweathered peridotites, the analysis of the Al and V concentrations may be indicative of Sc grades. Also, the occurrence of hematite-bearing, gabbro-derived laterites cutting across peridotite-derived, yellow lateritic horizons is likely associated with Sc over-enrichment localized within a few meters from the gabbro salbands. Field-based recognition of gabbro-derived laterites is relatively straightforward and may be taken into consideration for target ranking prior to drill testing.

In addition to the potential covalorisation of Ni, Co and Sc in peridotite-derived laterites, saprolitised amphibolites may represent attractive targets for primary Sc production. However, this study has shown that amphibolites exhibit large variations in their Sc content, both in unweathered facies and in their weathered derivatives, and that they represent discrete occurrences of relatively restricted volumes. Following the field-based recognition of amphibolite-bearing intrusions, the identification of fertile amphibolites may be based on textural observations determining the relative proportion and crystal size of hornblende, with preference for pegmatoïd textures. Also, analysis of Ti and V in amphibolites may provide first order estimates of their Sc content.

8. Conclusion

This contribution examines the distribution and the critical controls on the formation of Sc-rich zones within New Caledonian laterites. The yellow lateritic zones of some peridotite-derived Ni-laterites exhibit elevated Sc concentrations up to 100 ppm, suggesting potential for co-valorisation along with Ni and Co production. Spatially restricted, amphibolite-derived saprolites are also host to remarkable Sc concentrations up to > 300 ppm.

The initial Sc content of parent rocks represent the first critical control on the maximum Sc grades reached in their lateritised derivatives. In unweathered peridotites, enstatite is the dominant Sc host, controlling the Sc content of harzburgite and lherzolite. In intrusive mafic to ultramafic rocks, hornblende is the dominant Sc host, controlling the Sc content of hornblende-bearing intrusive rocks. In all investigated lateritic profiles, residual Sc enrichment in the upper, goethite-dominated horizons constitutes the second critical condition for the development of Sc-rich zones. Third, the expulsion of Sc from the uppermost horizons and downwards over-concentration following goethite recrystallisation and/or dehydration leads to further Sc enrichment. In peridotite-derived Ni laterites, the upgrade of the Sc content corresponds to a ~tenfold enrichment compared to the parent peridotite. The occurrence of elevated Sc concentrations up to 100 ppm in the yellow lateritic zones of harzburgite- and lherzolite-derived Ni-laterites suggests potential for co-valorisation along with Ni and Co production, providing that Sc-rich zones sufficiently overlap low-grade lateritic Ni(-Co) ore zones. In amphibolite-derived saprolites, Sc-bearing goethite yields Sc concentrations up to 800 ppm but occurs in association with gibbsite and/or kaolinite so that maximum bulk rock Sc concentrations only grades up to ~300 ppm, corresponding to a two- to threefold increase of the Sc content compared to the parent rock. Such concentrations may be economically attractive for standalone Sc production, although high-grade saprolitised amphibolites represent marginal volumes especially when compared to high-grade Sc deposits recognized in Australia (Chassé et al., 2017). Contrasting with peridotites and amphibolites, the lateritisation of gabbros leads to the preferential formation of hematite rather than goethite, resulting in significant remobilisation of Sc and subsequent trapping in the surrounding goethite-rich, peridotite-derived Ni laterite. There, over-enrichment up to >150-200 ppm may add significant value in the perspective of Ni-Co-Sc co-valorisation.

Acknowledgments

This work has been funded and logistically supported by the French National Research Agency through the national program “Investissements d’avenir” of the Labex Ressources 21 with the reference ANR-10-LABX-21-RESSOURCES21 and by the National Centre for Technological Research “Nickel et son environnement” based in New Caledonia. The authors would like to thank Dr. Brice Sevin, Stephane Lesimple and Dr. Bernard Robineau from the Geological Survey of New Caledonia, together with France Bailly and Laurence Barriller from the National Centre for Technological Research, for their technical and logistical support as well as for sharing their extensive knowledge of the geology of New Caledonia. We are grateful to Société Le Nickel (SLN), Koniambo Nickel SAS (KNS), Nickel Mining Company (NMC), Société des Mines de la Tontouta (SMT) and Mai Kouaoua Mines (MKM) for support and access to mines and drill cores. In particular, we acknowledge Dr. Mohamed Kadar (SLN), Dr. Clément Marcaillou (SLN), Dr. Maxime Drouillet (KNS), Willy Foucher (NMC), Mathieu Mazières (SMT), Matthieu Muret (SMT) and Matthieu Désesquelles (MKM) for their involvement. We also thank Dr. Christophe Cloquet (SARM analytical centre, CRPG, Vandœuvre-lès-Nancy, France), Dr. Marie-Christine Boiron, Dr. Chantal Peiffert, Dr. Andreï Lecomte and Dr. Olivier Rouer (GeoRessources, Vandœuvre-lès-Nancy, France) for technical support in providing analytical data.

References

Aiglsperger, T., Proenza, J.A., Lewis, J.F., Labrador, M., Svojtka, Rojas-Puron, A., Longo, F., Durisova, J. 2016. Critical metals (REE, Sc, PGE) in Ni laterites from Cuba and the Dominican Republic. Ore Geology Reviews 76 (1) 127-147.

Ambrosi, J.P., Nahon, D., Herbillon, A.J. 1986. The epigenetic replacement of kaolinite by hematite in laterite - Petrographic evidence and the mechanisms involved. Geoderma 37, 283-294.

Audet, M. 2008. Le massif du Koniambo, Nouvelle-Calédonie. Formation et obduction d'un complexe ophiolitique du type SSZ. Enrichissement en nickel, cobalt et scandium dans les profils résiduels. Ph.D thesis, université de la Nouvelle Calédonie / Université du Quebec à Montréal, 326 pp.

Avias, J. 1967. Overthrust structure of the main ultrabasic New Caledonian massives. Tectonophysics 4, 531–541.

Bailly, L., Ambrosi, J.P., Barbarand, J., Beauvais, A., Cluzel, D., Lerouge, C., Prognon, C., Quesnel, F., Ramanaïdou, E., Ricordel-Prognon, C., Ruffet, G., Sevin, B., Wells, L., Yans, J. 2014. Projet NICKAL: "Typologie des minerais latéritiques de Nouvelle-Calédonie et facteurs de concentration de Co et Ni", rapport final, BRGM/RP-63 482-FR, 402 pp.

Butt C.R.M., Cluzel D. 2013. Nickel laterite ore deposits: weathered serpentinites. Elements 9.123-128.

Cathelineau, M., Quesnel, B., Gautier, P., Boulvais, P., Couteau, C., Drouillet, M. 2016. Nickel dispersion and enrichment at the bottom of the regolith: formation of pimelite target-like ores in rock block joints (Koniambo Ni deposit, New Caledonia). Mineralium Deposita 51 (2), 271-282.

Cathelineau, M., Myagkiy, A., Quesnel, B., Boiron, M.-C., Gautier, P., Boulvais, P., Ulrich, M., Truche, L., Golfier, F., Drouillet, M. 2017. Multistage crack seal vein and hydrothermal Ni enrichment in serpentinized ultramafic rocks (Koniambo massif, New Caledonia). Mineralium Deposita 52 (7), 945-960.

Chassé, M., Griffin, W.L., O'Reilly, S.Y., Calas, G. 2017. Scandium speciation in a world-class lateritic deposit. Geochemical Perspectives Letters 3, 105–114.

Cluzel, D., Aitchison, J.C., Picard, C. 2001. Tectonic accretion and underplating of mafic terranes in the Late Eocene intraoceanic fore-arc of New Caledonia (Southwest Pacific): geodynamic implications. Tectonophysics 340 (1-2), 23-59.

Cluzel, D., Meffre, S., Maurizot, P., Crawford, A.J. 2006. Earliest Eocene (53 Ma) convergence in the Southwest Pacific: evidence from pre-obduction dikes in the ophiolite of New Caledonia. Terra Nova 18, 395–402.

Cluzel, D., Maurizot, P., Collot, J., Sevin, B. 2012a. An outline of the Geology of New Caledonia; from Permian–Mesozoic Southeast Gondwanaland active margin to Cenozoic obduction and supergene evolution. Episodes 35 (1), 72-86.

Cluzel, D., Jourdan, F., Meffre, S., Maurizot, P., Lesimple, S. 2012b. The metamorphic sole of New Caledonia ophiolite: 40Ar/39Ar, U-Pb, and geochemical evidence for subduction inception at a spreading ridge. Tectonics 31, 1-18.

Das, H.A., Zonderhuis, J., van der Marel, H.W. 1971. Scandium in rocks, minerals and sediments and its relations to iron and aluminium. Contributions to Mineralogy and Petrology 32 (3), 231-244.

Dublet, G., Julliot, F., Morin, G., Fritsch, E., Fandeur, D., Brown Jr., G.E. 2015. Geochimica et Cosmochimica Acta 160, 1–15.

Emsley, J. 2014. Unsporting Scandium. Nature Chemistry 6, 1025.

Freyssinet, P.H., Butt, C.R.M., Morris, R.C., Piantone, P. 2005. Ore-Forming Processes Related to Lateritic Weathering. In: Hedenquist JW, Thomson JFH, Goldfarb RJ, Richards JP (eds), Economic Geology 100th Anniversary Volume. Economic Geology Publishing Company, New Haven, Connecticut, pp. 681-722.

Genna, A., Maurizot, P., Lafoy, Y., Augé, T. 2005. Role of karst in the nickeliferous mineralisations of New Caledonia. Compte Rendus Geoscience 337 (3), 367-374.

Golightly, J.P. 2010. Progress in understanding the evolution of nickel laterites. In: Goldfarb RJ, Marsh EE, Monecke T (eds) The Challenge of Finding New Mineral Resources: Global Metallogeny, Innovative Exploration, and New Discoveries Volume II. Society of Economic Geologists Special Publication 15, pp. 451-475.

Guillong M.M., Maier D.L., Allan M.M., Heinrich C.A. 2008. SILLS: a MATLAB based program for the reduction of laser ablation ICPMS data of homogeneous materials and inclusions. Sylvester P (ed) Laser Ablation ICPMS in the Earth Sciences. Current Practices and Outstanding Issues, 328- 333.

Guillon, J. H. 1975. Les massifs péridotitiques de Nouvelle-Calédonie, Mémoires, vol. 76, 120 pp., ORSTOM, Paris.

Hoatson, D.M., Jaireth, S., Miezitis, Y. 2011. The major rare-earth-element deposits of Australia: geological setting, exploration, and resources. Geoscience Australia, 204 pp.

Latham, M. 1985. Altération et pédogenèse sur roches ultrabasique en Nouvelle Caledonie. Genèse et évolution des accumulations de fer et de silice en relation avec la formation du modéle, Thèse d'état, Dijon, 331 pp. ORSTOM.

Manceau, A., Schlegel, M.L., Musso, M., Sole, V.A., Gauthier, C., Petit, P.E., Trolard, F. 2000. Crystal chemistry of trace elements in natural and synthetic goethite. Geochimica et Cosmochimica Acta 64 (21), 3643–3661.

Maulana, A., Sanematmatmatsu, K., Sakakibara, M. 2016. An Overview on the Possibility of Scandium and REE Occurrence in Sulawesi, Indonesia. Indonesian Journal on Geoscience 3, 139–147.

Maurizot, P., Vendé-Leclerc, M. 2009. New Caledonia geological map, scale 1/500 000, Direction de l'Industrie, des Mines et de l'Énergie – Service de la Géologie de Nouvelle-Calédonie, Bureau de Recherches Géologiques et Minières.

Mortimer, N., Campbell, H.J., Tulloch, A.J., King, P.R., Stagpoole, V.M., Wood, R.A., Rattenbury, M.S., Sutherland, R., Adams, C.J., Collot, J., Seton, M. 2017. Zealandia: Earth's Hidden Continent. GSA Today 27 (3), 27-35.

Munoz, M., Ulrich, M. 2017. Distribution and speciation of Sc in lateritic profile of New Caledonia using synchrotron-XRF and Sc K-edge XANES spectroscopy. Geochemical cycle of Ni, Co and Sc: from mining exploration to ecotoxicity International Workshop October 17-19, 2017.

Orloff, O. 1968. Etude géologique et géomorphologique des massifs d'ultrabasites compris entre Houailou et Canala (Nouvelle-Calédonie), PhD thesis, Univ. Montpellier, France, 189 pp.

Paquette, J.L., Cluzel, D. 2007. U–Pb zircon dating of post-obduction volcanic-arc granitoids and a granulite-facies xenolith from New Caledonia. Inference on Southwest Pacific geodynamic models. International Journal of Earth Sciences 96 (4), 613-622.

Quesnel, B., Gautier, P., Boulvais, P., Cathelineau, M., Maurizot, P., Cluzel, D., Ulrich, M., Guillot, S., Lesimple, S., Couteau. C. 2013. Syn-tectonic, meteoric water-derived carbonation of the New Caledonia peridotite nappe, Geology 41, 1063–1066.

Prinzhofer, A., Nicolas, A., Cassard, D., Moutte, J., Leblanc, M., Paris, J.P., Rabinovitch, M. 1980. Structures in the new caledonia peridotites-gabbros: Implications for oceanic mantle and crust. Tectonophysics 69 (1-2), 85-112.

Ramanaidou, E.R. 1989. Genèse d'un gisement latéritique, Evolution supergène des itabirites Protérozoiques de la mine de fer de Capanema (Minas Gerais, Brésil), PhD thesis, University of Poitiers, 183 pp.

Royset, J., Ryum, N. 2005. Scandium in aluminium alloys, International Materials Reviews 50 (1), 19-44.

Rudnick, R.L., Gao, S. 2014. Composition of the Continental Crust. In: Holland, H., Turekian, K.K. (Eds.) Treatise on Geochemistry, 2nd Edition. Elsevier Ltd, Amsterdam, Netherlands, 1–51.

Schwertmann, U., Latham, M. 1986. Properties of iron oxides in some New Caledonian oxisols. Geoderma 39, 105-123.

Sevin, B., Ricordel-Prognon, C., Quesnel, F., Cluzel, D., Lesimple, S., Maurizot, P. 2012. First palaeomagnetic dating of ferricrete in New Caledonia: new insight on the morphogenesis and palaeoweathering of 'Grande Terre'. Terra Nova 24, 77-85.

Sevin, B., Cluzel, D., Maurizot, P., Ricordel-Prognon, C., Chaproniere, G., Folcher, N., Quesnel, F. 2014. A drastic lower Miocene regolith evolution triggered by post obduction slab break-off and uplift in New Caledonia. Tectonics 33 (9), 1787-1801.

Tardy, Y., Nahon, D. 1985. Geochemistry of laterites, stability of Al-goethite, Al-hematite and Fe^{3+}-kaolinite in bauxites and fericretes: an approach to the mechanism of concretion formation. American Journal of Science 285, 865-903.

Toropova, L.S., Eskin, D.G., Kharakterova, M.L., Dobatkina, T.V. 1998. Advanced Aluminium Alloys Containing Scandium. Structure and Properties, Gordon and Breach Science Publishers, Amsterdam, pp. 175.

Trescases, J.-J. 1975. L'evolution Géochimique Supergène des Roches Ultrabasiques en Zone Tropicale: Formation des Gisements Nickélifères de Nouvelle-Calédonie Edited, Paris, O.R.S.T.O.M., France.

Trolard, F., Tardy, Y. 1989. A model of Fe^{3+}-kaolinite-Al^{3+}-goethite-Al^{3+}-hematite equilibria in laterites. Clay Minerals 24, 1-21.

Ulrich, M., Picard, C., Guillot, S., Chauvel, C., Cluzel, D., Meffre, S. 2010. Multiple melting stages and refertilization as indicators for ridge to subduction formation: The New Caledonia ophiolite. Lithos 115, 223-236.

Ulrich, M. 2010. Péridotites et serpentinites du complexe ophiolitique de la Nouvelle-Calédonie. PhD thesis, Université Joseph Fournier – Université de la Nouvelle-Calédonie, 272 pp.

Ulrich M., Cathelineau M., Boiron M.-C., Muñoz M., Teitler Y. In prep. LA-ICP-MS analysis of Scandium: calibration, and application to in situ analysis of Sc in silicates and oxides. Submitted to Journal of Geochemical Exploration.

U.S. Geological Survey (2016) Scandium. In: Mineral Commodity Summaries. U.S. Geological Survey, Reston, USA, 146–147.

Wells, M.A., Ramanaidou, E.R., Verrall, M., Tessarolo, C. 2009. Mineralogy and crystal chemistry of "garnierites" in the Goro lateritic nickel deposit, New Caledonia. European Journal of Mineralogy 21 (2), 467-483.